TGFβ restores hematopoietic homeostasis after myelosuppressive chemotherapy

Fabienne Brenet,[1,2] Pouneh Kermani,[1,5] Roman Spektor,[1,2] Shahin Rafii,[4] Joseph M. Scandura[1,2,3]

[1]Department of Medicine, Division of Hematology/Oncology; [2]Laboratory of Molecular Hematopoiesis; [3]Leukemia Program; [4]Howard Hughes Medical Institute, Department of Genetic Medicine and Ansary Stem Cell Institute; and [5]Department of Cell and Developmental Biology, Weill Cornell Medical College, New York, New York 10065

Myelosuppression is a life-threatening complication of antineoplastic therapy, but treatment is restricted to a few cytokines with unilineage hematopoietic activity. Although hematopoietic stem cells (HSCs) are predominantly quiescent during homeostasis, they are rapidly recruited into cell cycle by stresses, including myelosuppressive chemotherapy. Factors that induce HSCs to proliferate during stress have been characterized, but it is not known how HSC quiescence is then reestablished. In this study, we show that TGFβ signaling is transiently activated in hematopoietic stem and progenitor cells (HSPCs) during hematopoietic regeneration. Blockade of TGFβ signaling after chemotherapy accelerates hematopoietic reconstitution and delays the return of cycling HSCs to quiescence. In contrast, TGFβ blockade during homeostasis fails to induce cycling of HSPCs. We identified the cyclin-dependent kinase inhibitor Cdkn1c (p57) as a key downstream mediator of TGFβ during regeneration because the recovery of chimeric mice, incapable of expressing p57 in HSPCs, phenocopies blockade of TGFβ signaling after chemotherapy. This study demonstrates that context-dependent activation of TGFβ signaling is central to an unrecognized counterregulatory mechanism that promotes homeostasis once hematopoiesis has sufficiently recovered from myelosuppressive chemotherapy. These results open the door to new, potentially superior, approaches to promote multilineage hematopoietic recovery by blocking the TGFβ signaling that dampens regeneration.

CORRESPONDENCE
Joseph M. Scandura:
jms2003@med.cornell.edu

Abbreviations used: 5FU, 5-fluorouracil; CDKI, cyclin-dependent kinase inhibitor; CMP, common myeloid progenitor; FLMC, fetal liver mononuclear cell; GMP, granulocyte macrophage progenitor; HPC, hematopoietic progenitor cell; HSC, hematopoietic stem cell; HSPC, hematopoietic stem and progenitor cell; IF, immunofluorescence; IHC, immunohistochemical; LAP, latency-associated peptide; Lin^-, hematopoietic cells not expressing mature lineage markers; LKS^+ cells, $Lin^-/cKit^+/Sca\text{-}1^+$ cells; LKS + SLAM cells, $LKS^+/CD150^+/CD48^-$ cells; LT-HSCs, long-term HSCs; MEP, megakaryocyte erythroid progenitor; MPP, multipotent progenitor cell; pSmad2, phosphorylated Smad2.

Hematopoietic stem cells (HSCs) are required for lifelong blood cell production and, to prevent exhaustion, the majority of HSCs are deeply quiescent during steady-state hematopoiesis (Bradford et al., 1997; Cheshier et al., 1999; Passegué et al., 2005). Paracrine factors produced by specialized BM niche cells maintain HSC quiescence (Wilson and Trumpp, 2006; Ehninger and Trumpp, 2011; Lévesque and Winkler, 2011). During hematologic stress, HSCs are rapidly recruited into cell cycle and undergo extensive self-renewal and differentiation to meet increased hematopoietic demands. A great deal is known about how HSCs are mobilized during these periods of stress. Proteolytic enzymes such as matrix metalloproteinase-9, cathepsin G, and elastase cleave the chemokines (e.g., CXCL12), cytokines (e.g., KITL), and adhesive interactions that retain HSCs in the niche and maintain their quiescence (Heissig et al., 2002; Lapidot and Petit, 2002; Petit et al., 2002; Lévesque et al., 2003; Kopp et al., 2005; Kollet et al., 2006). Circulating cytokine levels increase in response to cytopenias, tissue injury, and inflammation and this reinforces hematopoietic stem and progenitor cell (HSPC) proliferation. Yet it is not known how these processes wind down to allow HSCs to withdraw from cell cycling and return to quiescence. To challenge the tacit paradigm that homeostasis is passively reestablished as stress mediators normalize, and because TGFβ can block cytokine-driven HSC cycling, we examined the possibility that activation of the TGFβ pathway might dampen hematopoietic recovery after stress (Batard et al., 2000; Scandura et al., 2004; Yamazaki et al., 2009).

TGFβ is one of the most potent inhibitors of cytokine-driven HSC proliferation in vitro

The Rockefeller University Press $30.00
J. Exp. Med. 2013 Vol. 210 No. 3 623-639
www.jem.org/cgi/doi/10.1084/jem.20121610

(Batard et al., 2000; Blank and Karlsson, 2011; Fortunel et al., 2000a,b; Scandura et al., 2004; Sitnicka et al., 1996), but its role in hematopoiesis has been harder to establish (Capron et al., 2010; Dickson et al., 1995; Larsson et al., 2003; Larsson et al., 2005; Larsson et al., 2001; Oshima et al., 1996). Identifying HSC defects in knockouts of TGFβ1, or of its receptors Tgfbr1 (Alk5) and Tgfbr2, was difficult because the engineered mice develop a transplantable, lethal inflammatory disorder that largely prevents analysis of steady-state hematopoiesis in adult mice (Gorelik and Flavell, 2000; Letterio et al., 1996; Levéen et al., 2002; Yaswen et al., 1996). Nonetheless, recent studies using a variety of elegant approaches to circumvent this lethal inflammatory disorder strongly suggest that TGFβ, signaling through Tgfbr2 and recruiting Smad4, is a putative niche factor that can maintain HSC quiescence during steady-state hematopoiesis (Blank et al., 2006; Yamazaki et al., 2006, 2009, 2011; Karlsson et al., 2007). Yet differences between the in vitro and in vivo effects of TGFβ on hematopoietic cells and the disparate phenotypes of mice with targeted deletion of TGFβ ligands or their cognate receptors suggest that the effects of TGFβ signaling are context dependent.

Here, we show that TGFβ pathway activation marks regenerating HSPCs returning to quiescence and that this context-dependent signaling helps reestablish homeostasis during recovery from chemotherapy. This finding has immediate clinical relevance because TGFβ blockade in this setting promotes multilineage hematopoietic regeneration by prolonging HSPC cycling and promoting self-renewal. Together, our data demonstrate that myelosuppression drives hematopoiesis using not only a cytokine-fueled gas pedal but also taps an active braking mechanism once sufficient recovery has been attained.

RESULTS

TGFβ signaling is activated during hematopoietic recovery from myelosuppression

To study hematopoietic recovery after chemotherapy, we treated mice with the antimetabolite 5-fluorouracil (5FU) and measured TGFβ1 in the BM during hematopoietic regeneration (Fig. 1 B). 5FU targets cycling hematopoietic cells and causes extensive BM aplasia with a nadir between days 6 and 8 after chemotherapy. The level of active TGFβ (ELISA) initially declined slightly but then rose significantly as hematopoiesis was restored 11–15 d after chemotherapy. We monitored phosphorylation of the intracellular mediator Smad2 (pSmad2), to report downstream activation of the TGFβ pathway. Whereas immunohistochemical (IHC) staining for pSmad2 was weak in homeostatic BM (5FU-D0), both the intensity and proportion of BM cells staining for pSmad2 increased during hematopoietic regeneration after chemotherapy (Fig. 1, A and B). Smad2 phosphorylation peaked on day 15 when the BM cellularity and blood counts were returning to normal. Western blots confirmed strong induction of TGFβ signaling on day 15 in immature, Lin^- (not expressing mature lineage markers) hematopoietic cells isolated from the marrow or spleen (Fig. 1 C). We sorted LKS^+ cells (Lin^-, $cKit^+$, $Sca\text{-}1^+$) highly enriched for HSPCs onto coverslips before and on day 15 after a myelosuppressive dose of 5FU and used immunofluorescence (IF) staining and confocal microscopy to quantify relative pSmad2 expression (Fig. 1, D and E). These results show that TGFβ is activated within the BM and its intracellular signaling is induced in HSPCs during late hematopoietic regeneration. Because TGFβ signaling was activated in HSPCs when hematopoiesis was being replenished, we tested the hypothesis that blockade of this pathway would affect hematopoietic regeneration.

TGFβ blockade after chemotherapy promotes hematopoietic regeneration

To assess how TGFβ signaling alters hematopoietic regeneration, we administered myelosuppressive chemotherapy to mice, and then, during recovery, treated cohorts with either an antibody that specifically neutralizes active TGFβ (1D11), an isotype control antibody (13C4), or nothing at all (control; Fig. 2 A). Inhibition of TGFβ signaling by 1D11 during regeneration by 1D11 was confirmed by Western blot of Lin^- cells before and on day 15 after chemotherapy (Fig. 2 B). Multilineage hematopoiesis regenerated more quickly in mice treated with 1D11 than it did in either control group (Fig. 2, C and E). The effect of TGFβ blockade could not result from altered chemotherapy cytotoxicity because the inhibitor was administered after the BM cellularity had already reached nadir. Because both myeloid (RBC, PLTs, and the granulocytic subpopulation of WBCs [not depicted]) and lymphoid lineages (the lymphoid subpopulation of WBCs; not depicted) recovered faster in the mice treated with the TGFβ neutralizing antibody, we reasoned that the accelerated recovery was likely a consequence of enhanced HSPC regeneration and indeed we found more immature, Lin^- cells during regeneration of the marrow in mice treated with the inhibitor (unpublished data). Notably, blockade of TGFβ in untreated, steady-state BM did not increase blood cell counts or BM cellularity (Fig. 2 F), demonstrating that the effect of TGFβ blockade is context dependent. These studies suggest that activation of the TGFβ pathway restrains hematopoietic regeneration after myelotoxic stress.

Context-dependent TGFβ signaling restores HSPC quiescence and limits self-renewal after chemotherapy

To investigate the mechanisms by which TGFβ dampens hematopoietic recovery, we used polyvariate flow cytometry to analyze HSPC regeneration in mice treated with chemotherapy followed by either 1D11 or the 13C4 control antibody (Fig. 3 A). Ordinarily, myelotoxic stress triggers self-renewal of HSCs coupled to expansion of hematopoietic progenitor cells (HPCs; Morrison et al., 1997; Passegué et al., 2005; Wilson et al., 2008). We found greater expansion of total LKS^+ cells and enriched LKS^+ subsets ($LKS^+CD34^-FLK2^-$, $LKS^+CD34^+FLK2^-$, and $LKS^+CD150^+CD48^-$) in mice treated

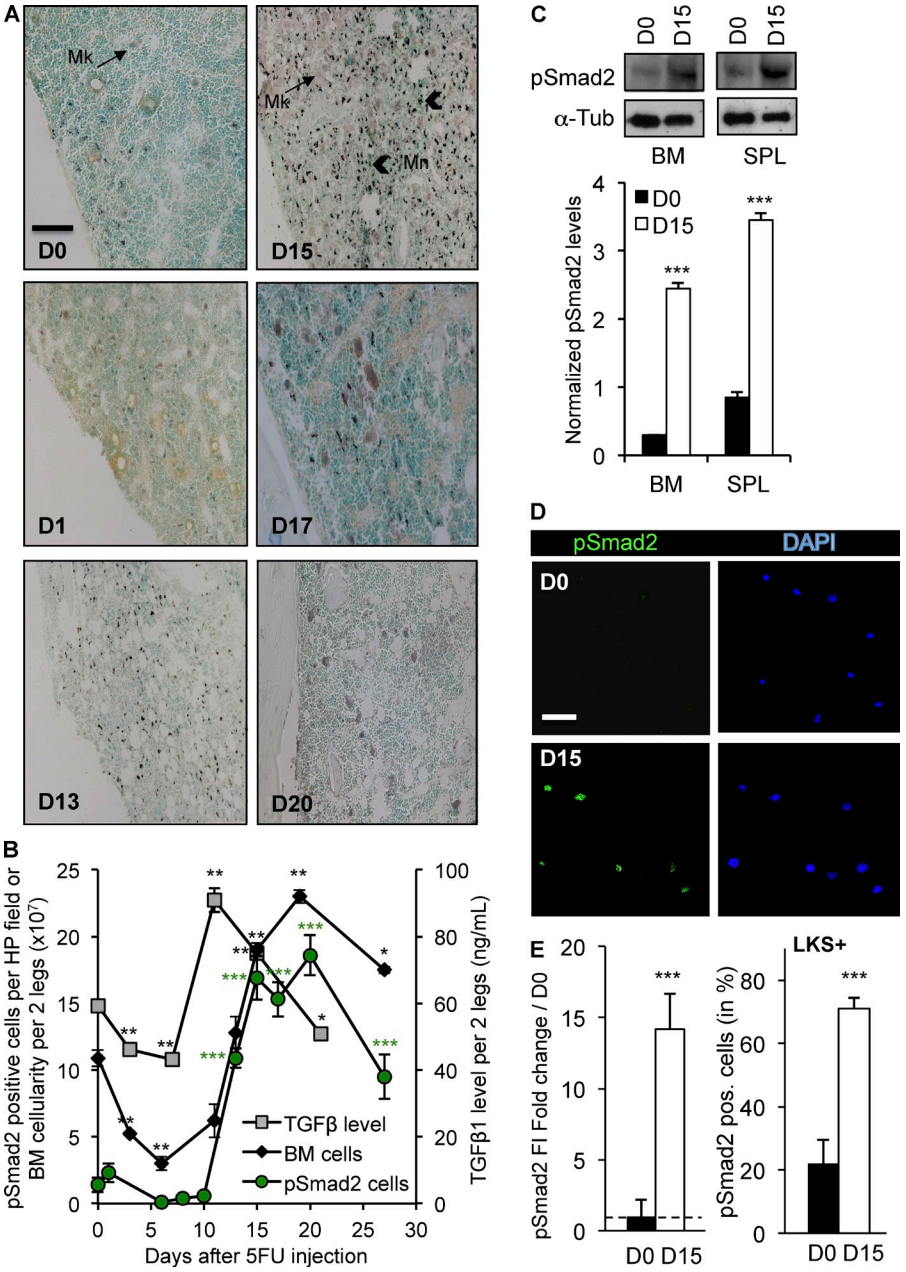

Figure 1. TGFβ signaling is activated during BM recovery from chemotherapy. WT mice (n = 16) were treated with a single dose of 5FU (250 mg/kg, i.p.) on day 0. (A) IHC staining for pSmad2 was performed on BM sections collected before and after chemotherapy. Sections were counterstained with the nuclear stain, methyl green, to assess cellularity (bar, 100 µm). (B) ELISA measurement of active TGFβ in the BM (gray squares), quantification of pSmad2-positive cells per high-power (HP) IHC field (green circles) and BM cellularity (black diamonds) were assessed before (D0) and at the indicated times after chemotherapy. (C; top) Representative immunoblot of pSmad2 (~55-kD) in Lin$^-$ BM and spleen cells during homeostasis (D0) and during recovery from chemotherapy (D15). (bottom) Replicate blots were quantified using ImageJ and pSmad2 was normalized to the α-tubulin (~50 kD) loading control (n = 3). (D) FACS-purified LKS$^+$ cells were stained for pSmad2 (green) and DAPI (blue) on day 0 and 15 (bar, 50 µm). (E) pSmad2 fluorescence intensity (FI) was quantified using ImageJ software. The day 15/day 0 FI ratio (left) and the percentage of pSmad2$^+$ LKS$^+$ cells are shown at day 0 and 15 (right). All experiments were performed at least twice, usually three to five times. All quantified data are shown as mean ± SEM (*, $P < 0.05$; **, $P < 0.01$; ***, $P < 0.001$, or if undesignated, the comparison was not significant).

with 1D11 (Fig. 3, A and B). There were also more colony-forming cells (CFCs) and LKS$^-$ HPCs in the BM of mice that had TGFβ signaling blocked during regeneration after chemotherapy (Fig. 3, C and E; and not depicted). Notably, regeneration of very immature LKS + SLAM (LKS$^+$, CD150$^+$, CD48$^-$) cells—an immunophenotype highly enriched for HSCs during homeostasis and stress (Kiel et al., 2005; Yilmaz et al., 2006)—was also enhanced in mice treated with the TGFβ-neutralizing antibody (Fig. 3 D). To assess whether TGFβ blockade expanded bona fide HSCs with long-term repopulation potential relative to controls, we performed competitive transplantation assays. We isolated cells from the BM of D15-I and D15-C EGFP$^{+/+}$ or CD45.1$^{+/+}$ mice (Fig. 2 A), mixed them in a 1:1 ratio, and then competitively transplanted them into normal recipients (Fig. 3 F). We monitored the contribution of the engrafted cells to multi-lineage blood cells using flow cytometry and markers of donor cell source (CD45.1, CD45.2, and EGFP; Fig. 3 G). Although initial engraftment was in the expected proportion, the contribution of D15-I cells progressively overtook that of D15-C cells. The time frame of the competitive advantage suggests that TGFβ blockade after chemotherapy promoted the expansion of cells with long-term repopulation potential. Therefore, in the absence of TGFβ, HSPCs undergo additional rounds of cell division during BM regeneration. We therefore reasoned that TGFβ might be directly involved in reestablishing HSPC quiescence.

We explored the mechanism by which TGFβ blockade enhances hematopoietic regeneration and promotes HSC

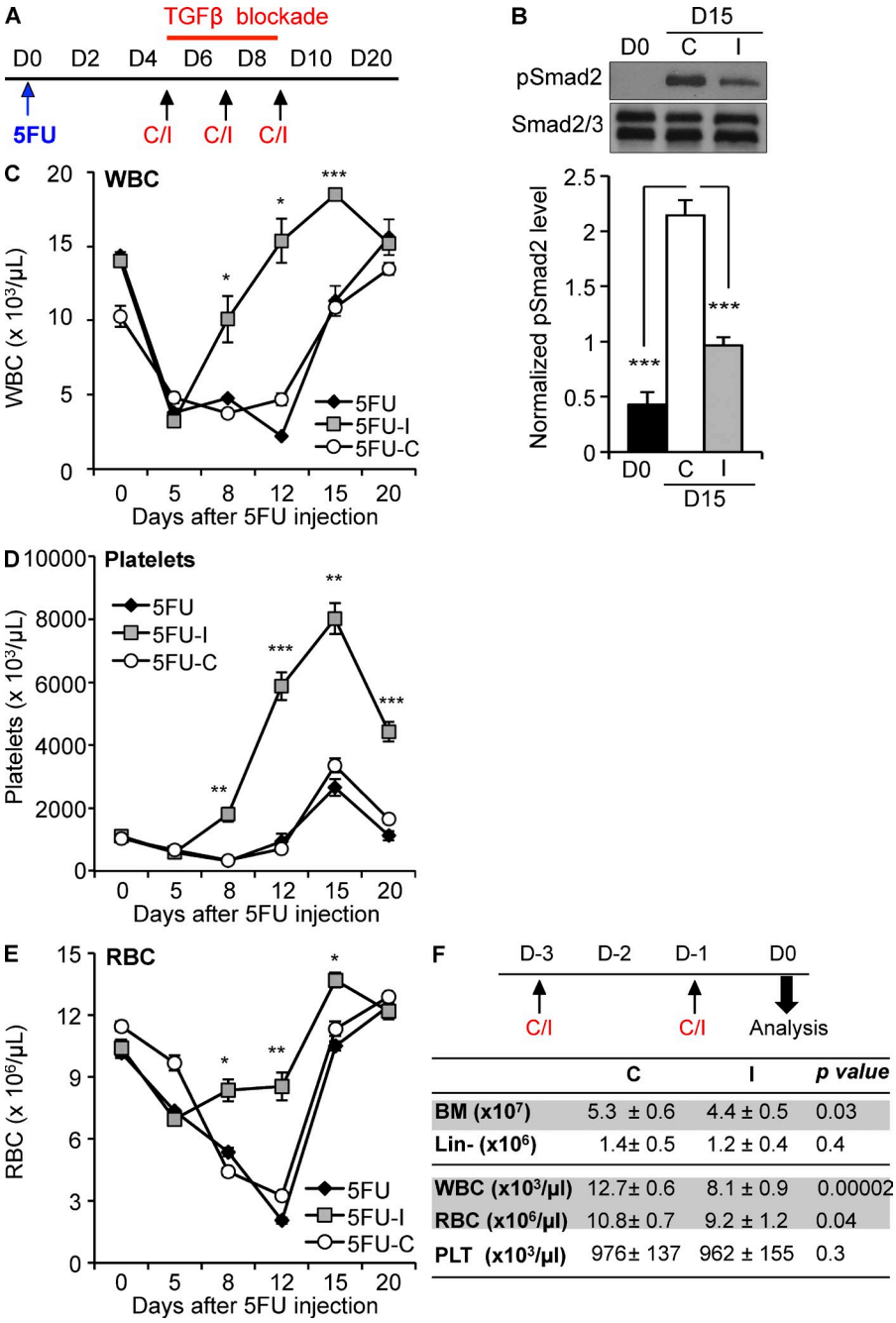

	C	I	p value
BM (x10⁷)	5.3 ± 0.6	4.4 ± 0.5	0.03
Lin- (x10⁶)	1.4± 0.5	1.2 ± 0.4	0.4
WBC (x10³/μl)	12.7± 0.6	8.1 ± 0.9	0.00002
RBC (x10⁶/μl)	10.8± 0.7	9.2 ± 1.2	0.04
PLT (x10³/μl)	976± 137	962 ± 155	0.3

Figure 2. Blockade of TGFβ during recovery from chemotherapy promotes hematopoietic regeneration. (A) Cohorts of mice were treated with 5FU on day 0, and then with no additional agent (black diamonds, 5FU), the TGFβ-neutralizing antibody, 1D11 (gray squares, 5FU-I), or a nontargeted isotype control antibody, 13C4 (white circles, 5FU-C; $n = 6$) on day 5, 7, and 9 (arrows). (B; top) Representative immunoblot of pSmad2 in Lin$^-$ BM during homeostasis (D0) and during recovery from chemotherapy (D15) with 1D11 (I) or 13C4 (C) antibody treatment. (bottom) Replicate blots were quantified using ImageJ and pSmad2 (~55 kD) was normalized to the Smad2 band (top) of the Smad 2/3 (~55/50 kD) loading control ($n = 3$). (C–F) Recovery of WBCs (C), platelets (D), and RBCs (E) is shown for treated mice ($n = 6$). (F) Cohorts of untreated, homeostatic mice ($n = 10$) were administered either the TGFβ-neutralizing antibody 1D11 (I; 10 mg/kg) or 13C4 control (C; 10 mg/kg) on days −3, −1 before analysis on day 0. Total BM cellularity and Lin-depleted cell count, WBCs, RBCs, and platelets (PLTs) were assessed after treatment. All quantified data are shown as mean ± SEM (*, $P < 0.05$; **, $P < 0.01$; ***, $P < 0.001$, or if undesignated, the comparison was not significant).

self-renewal by assessing the cell cycle status of HSPCs during recovery from myelosuppressive chemotherapy (Fig. 4). During steady-state hematopoiesis, most LKS$^+$ and LKS + SLAM cells are quiescent and bi-dimensional cell cycle analysis identifies them in G_0 (2N DNA with no Ki67; Passegué et al., 2005). After a myelotoxic insult, virtually all LKS$^+$ cells quickly enter cell cycle and continue to cycle until the BM begins to regenerate some time between day 13 and 15 (Fig. 4, A and B). Although HSPCs normally return to quiescence at this point, we found that TGFβ blockade permits LKS$^-$ HPCs (unpublished data), LKS$^+$ cells (Fig. 4 B) and LKS + SLAM cells (Fig. 4 C) to continue cycling for several more days. Similarly, mice treated with a small molecule inhibitor of Tgfbr1 (LY364947) after 5FU also had prolonged cycling of these cell populations and recovered blood counts more rapidly than did mice treated with a vehicle control (unpublished data). Thus, a previously unrecognized function of TGFβ is to reestablish HSC quiescence and restrain progenitor proliferation once hematopoiesis has sufficiently recovered from stress.

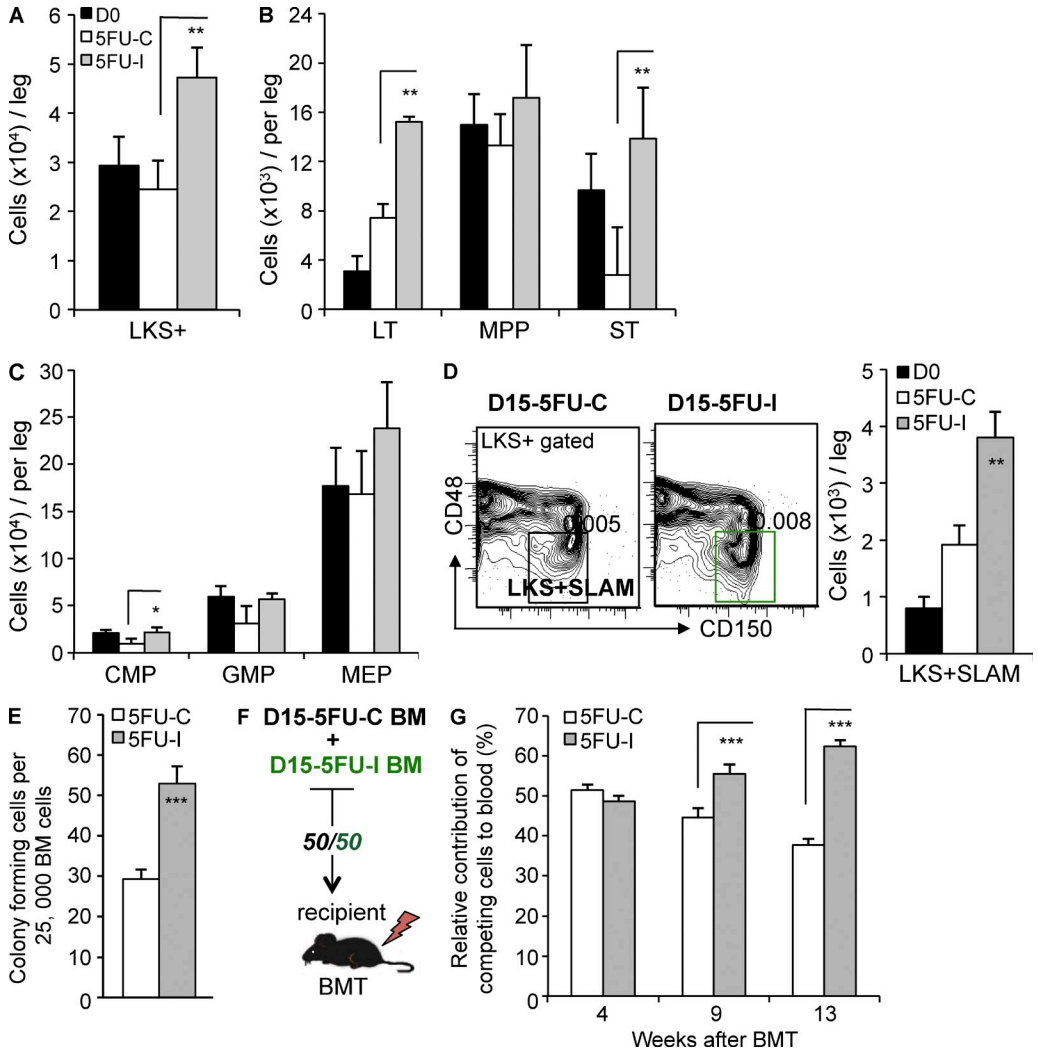

Figure 3. TGFβ limits HSPC proliferation after chemotherapy. (A–D) BM cell counts before (D0) and after (D15) treatment with 5FU and the TGFβ-neutralizing antibody, 1D11 (D15-I), or the control antibody (D15-C) were assessed by flow cytometry. Results were normalized per leg (femur + tibia) as indicated. Expansion of LKS$^+$ (Lin$^-$cKit$^+$Sca1$^+$) cells (A), LKS$^+$Flk2$^-$CD34$^-$ (LT), LKS+Flk2$^-$CD34$^+$ (ST), and LKS$^-$FCRγII/IIIdimCD34$^+$ CMPs and LKS + SLAM cells (D, right) is shown for untreated mice (black bars, D0) and mice treated with 5FU, and then 1D11 (gray bars, 5FU-I) or the control antibody (white bars, 5FU-C) during hematopoietic regeneration ($n = 5$). (D, left) Representative flow cytometry of LKS + SLAM (LKS$^+$CD48$^-$CD150$^+$) on day 15 after treatment with 5FU and either 1D11 (D15-I) or the control antibody (D15-C) is shown. (E) CFC assay for committed HPCs in D15-I BM and D15-C BM ($n = 3$). (F) Schematic of competitive repopulation analysis. EGFP or CD45.1-marked D15-C BMMC were mixed 1:1 with reciprocally marked D15-I BMMCs, and then transplanted into lethally irradiated recipient mice ($n = 10$). (G) Competitive repopulation by D15-C and D15-I cells of multilineage peripheral blood was analyzed by flow cytometry at the indicated times after transplantation ($n = 10$). All quantified data are shown as mean ± SEM (*, $P < 0.05$; **, $P < 0.01$; ***, $P < 0.001$, or if undesignated, the comparison was not significant).

To test whether this function depends on the circumstances of TGFβ blockade, we administered the 1D11 (inhibiting) or the 13C4 (control) antibody to untreated, homeostatic mice. Blockade of the TGFβ pathway during steady-state hematopoiesis failed to induce either LKS$^+$ cells (not depicted) or LKS + SLAM cells to emerge from quiescence (Fig. 4 D). This finding suggests that the action of TGFβ in homeostatic BM differs from that during late hematopoietic regeneration when the levels of active TGFβ increase and its downstream signaling in HSPCs manifests. These results indicate that a central role of TGFβ is to reestablish quiescence in the context of BM regeneration.

TGFβ induces context-dependent p57 expression during hematopoietic regeneration

To identify how spatiotemporal activation of TGFβ signaling reinstates quiescence of cycling HSPCs, we investigated the expression of cyclin-dependent kinase inhibitors (CDKIs) that function in these cells (p21/Cdkn1a, p27/Cdkn1b, p57/Cdkn1c, and p18/Cdkn2d; Cheng et al., 2000a,b; Scandura et al., 2004; Yuan et al., 2004; Matsumoto et al., 2011; Zou et al., 2011). Of these CDKIs, only p57 and p18 are induced in Lin$^-$ cells during the window of TGFβ activation (Fig. 5 A). We previously found that only p57—and not p18—was

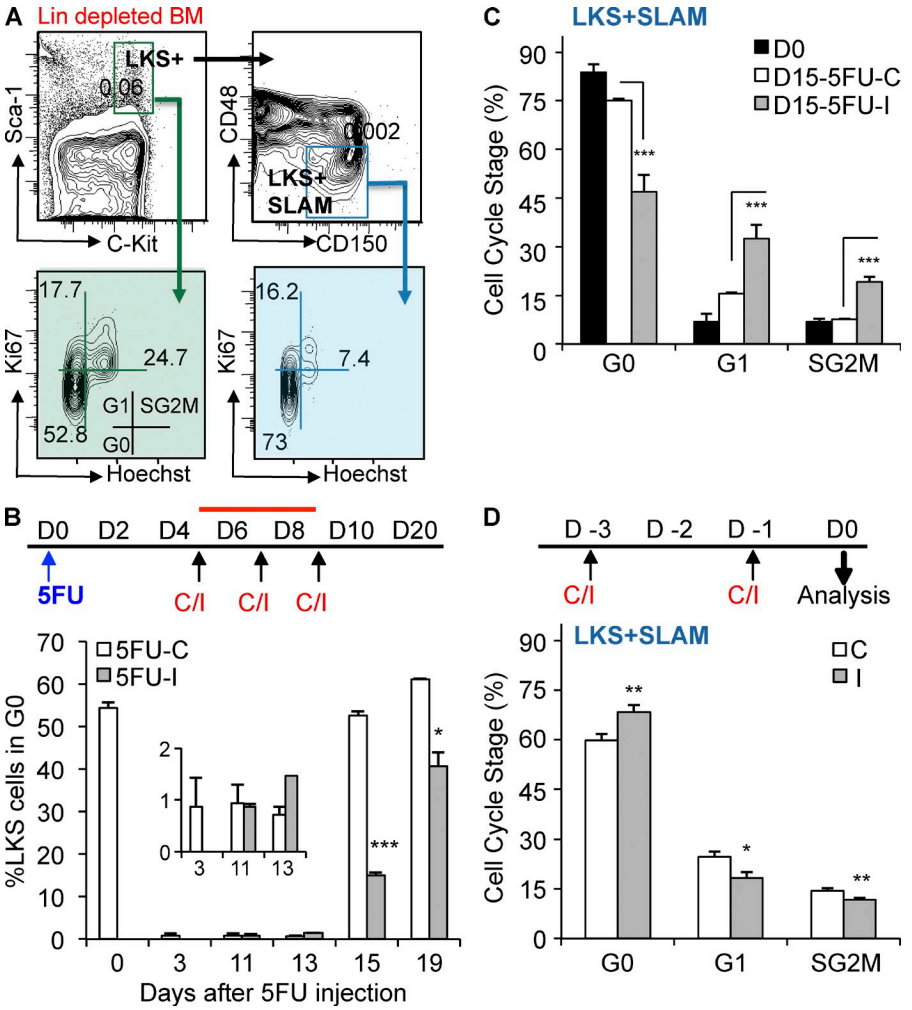

Figure 4. Blockade of TGFβ during recovery from myelotoxic stress prolongs HSPC cycling. (A) Flow cytometry gating strategy for cell cycle analysis of LKS$^+$ ($Lin^-cKit^+Sca1^+$) and LKS + SLAM ($Lin^-cKit^+Sca1^+CD48^-CD150^+$) cells is shown (top images show frequency in total BM; bottom images show percentage of LKS + SLAM gated cells). (B) Mice were treated with 5FU, and then with the TGFβ-neutralizing antibody, 1D11 (5FU-I), or the isotype control antibody 13C4 (5FU-C) on day 5, 7, and 9. The percentage of quiescent LKS$^+$ cells is shown before treatment (D0) and at various times after treatment with 5FU and 1D11 (5FU-I, gray bars) or the control antibody (5FU-C, white bars; $n = 5$/group). (C) Cell cycle status of BM LKS + SLAM HSCs is shown before (D0) and on day 15 after treatment with 5FU and 1D11 (5FU-I) or the control antibody ($n = 5$). (D) Cohorts of untreated, homeostatic mice ($n = 10$) were administered either the TGFβ-neutralizing antibody 1D11 (I; 10 mg/kg) or control antibody 13C4 (C; 10 mg/kg) on days −3 and −1 before analysis on day 0. Bivariate cell cycle status of BM LKS + SLAM HSC on day 0 is shown. All quantified data are shown as mean ± SEM (*, $P < 0.05$; **, $P < 0.01$; ***, $P < 0.001$, or if undesignated, the comparison was not significant).

transcriptionally regulated by TGFβ in human HSPCs, and we identified p57 as a major downstream mediator of TGFβ-induced cytostasis in these cells (Scandura et al., 2004). Subsequent work has shown that p57 is highly expressed in deeply quiescent HSCs ($CD34^-$ LKS), positioning this CDKI in a cellular compartment where it could function as a gatekeeper of quiescence (Yamazaki et al., 2006, 2009; Miyamoto et al., 2007; Qian et al., 2007). Indeed, p57 has been recently reported to help maintain HSC quiescence during steady-state hematopoiesis (Matsumoto et al., 2011; Zou et al., 2011). We therefore reasoned that p57 might also be a key effector of TGFβ, serving to reestablish HSC quiescence during late hematopoietic regeneration after chemotherapy.

IHC staining showed that the spatiotemporal pattern of p57 expression was similar to TGFβ pathway activation during BM regeneration (Fig. 5 B). During homeostasis in untreated mice, p57 expression is restricted to large, polyploidy megakaryocytes (Mk) and small, uncommon mononuclear cells (Mn), presumably HSPCs. During recovery from chemotherapy, the number of small p57-expressing cells increases dramatically and is most prominent on day 15. Western blots of immature Lin^- BM cells from 5FU-treated mice revealed strong up-regulation on day 15 of p57 and pSmad2 and, to a far less extent, of p27 (Fig. 5, C and D). Both Smad2 phosphorylation and p57 expression were blocked in Lin^- cells from mice treated with the TGFβ-neutralizing antibody 1D11, supporting a mechanistic link between TGFβ activation and p57 induction. In contrast, TGFβ blockade did not affect p27 up-regulation, confirming that p27 is neither a TGFβ target nor a central mediator of HSC quiescence during BM recovery (Cheng et al., 2001; Scandura et al., 2004).

To further explore the linkage between p57 expression and activation of TGFβ signaling, we FACS-isolated LKS$^+$ cells before and during recovery from chemotherapy in mice treated with 5FU, and then either the TGFβ-neutralizing antibody (1D11) or the control antibody (13C4). We then stained purified LKS$^+$ cells for p57 and pSmad2. As previously reported by others, we found p57 expression almost exclusively in the LKS$^+$ compartment in steady-state hematopoiesis (unpublished data). Only a subset of these homeostatic LKS$^+$ cells express p57 (Yamazaki et al., 2006) and staining for pSmad2 is weak in these cells suggesting that

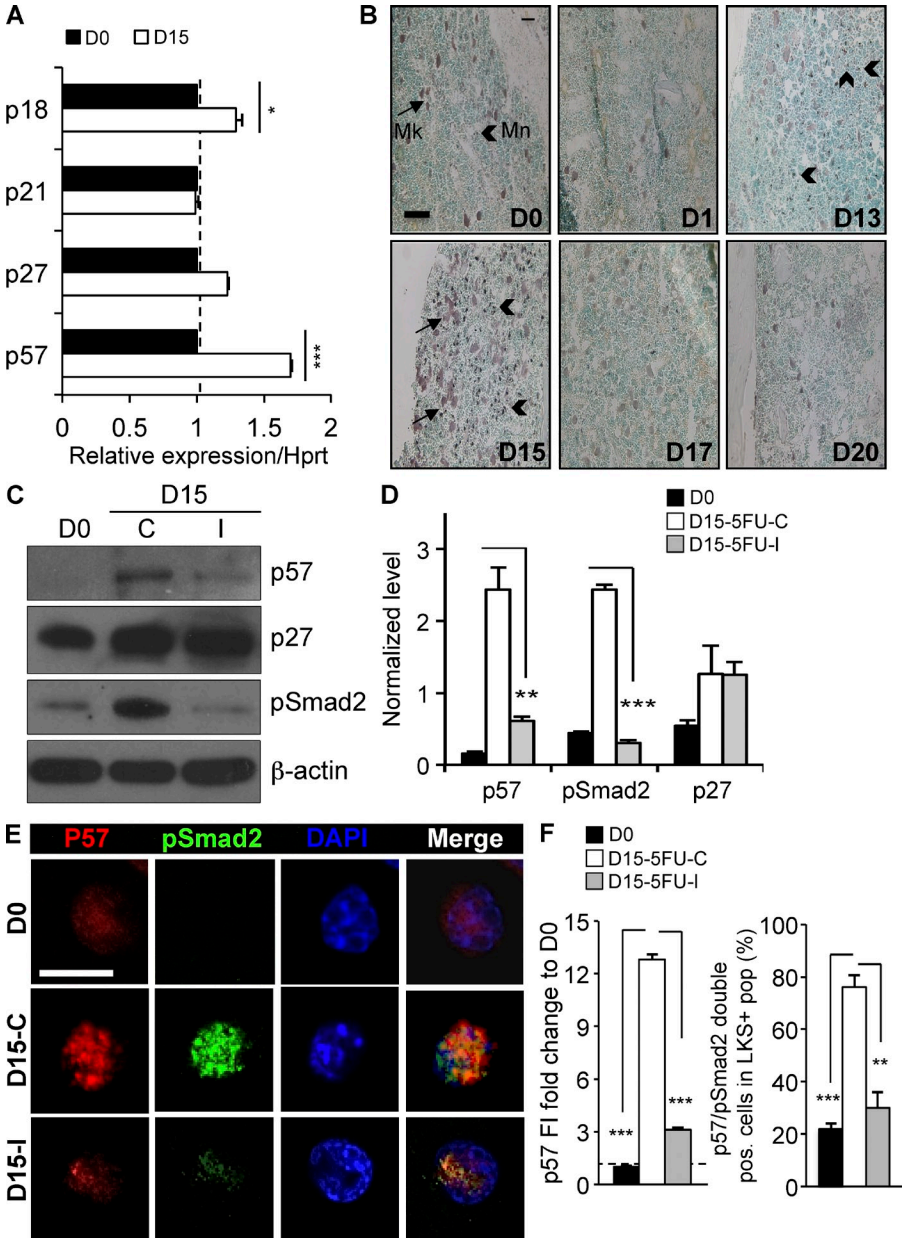

Figure 5. TGFβ is required for p57 up-regulation during recovery from myelosuppressive chemotherapy. (A) The expression of CDKIs in Lin⁻ BM cells of C57BL/6J mice before (D0) or after (D15) administration of 5FU (250 mg/kg, i.p.) was assessed by qRT-PCR. Expression of *p57*, *p21*, *p18*, and *p27* mRNA was normalized to *Hprt1* at each time point ($n = 3$). (B) Wild-type mice were killed before (D0) and at the indicated times after a single dose of 5FU chemotherapy. Femurs were stained by IHC for p57 and nuclei were counterstained with Methyl Green. p57 staining was seen in both megakaryocytes (Mk, small arrows) and small mononuclear cells (Mn, large arrow heads). Expression of p57 (reddish-brown) was maximally up-regulated 15 d after 5FU treatment (bar, 100 µm). (C) Cohorts of mice were treated with 5FU on day 0, and then with the TGFβ-neutralizing antibody 1D11 or a non-targeted control antibody 13C4 on day 5, 7, and 9. Immunoblots are shown for p57 (~51 kD), pSmad2 (~55 kD), and p27 (~27 kD), in Lin⁻ BM cells. (D) Replicate blots were quantified using ImageJ and expression normalized to β-actin (~45 kD; $n = 3$). (E) LKS⁺ cells were FACS purified from mice before (D0), and on day 15 after 5FU chemotherapy, followed by either 1D11 (D15-I) or 13C4 (D15-C), as described previously. Purified cells were stained for p57 (red), pSmad2 (green), and for DNA using DAPI (blue). Images were acquired using a Zeiss 710 laser scanning confocal microscope and (F) fluorescence intensity (FI) was quantified using ImageJ software (bar, 10 µm). All quantified data are shown as mean ± SEM (*, $P < 0.05$; **, $P < 0.01$; ***, $P < 0.001$, or if undesignated, the comparison was not significant).

other signaling pathways may regulate p57 expression during homeostasis (Yoshihara et al., 2007). In contrast, both p57 and pSmad2 significantly increased during recovery from hematopoietic stress in LKS⁺ cells isolated from mice treated with the control antibody but not in those treated with the 1D11 TGFβ-neutralizing antibody (Fig. 5, E and F). These results show that during recovery from chemotherapy, p57 is a downstream target of TGFβ in HSPCs.

p57 deletion has modest effect on homeostatic hematopoiesis

To test whether up-regulation of p57 is necessary for the cytostatic effects of TGFβ, we studied an engineered mouse strain that does not express p57 (Zhang et al., 1997). Of all the CDKIs, p57 is the only one required for life. Mice without p57 (p57-KO) die shortly after birth, usually as a result of poor feeding resulting from a cleft palate or other developmental abnormalities. We first generated an EGFP-expressing strain of mice that carried a paternally inherited p57-null allele (Schaefer et al., 2001). To study p57-KO hematopoiesis, we transplanted fetal liver mononuclear cells (FLMCs) obtained from p57-WT and p57-KO littermates (EGFP⁺) into lethally irradiated C57BL/6J recipient mice and allowed them to reach homeostasis. We did not identify significant differences in the number of FLMCs from p57-WT or p57-KO littermates, and the chimeric mice engrafted with p57-WT or p57-KO littermate FLMCs had similar BM cellularity and frequency of LKS⁺ cells at steady state (Fig. 6 A). HSPCs

deficient in p57 (p57-KO) engrafted normally and yielded durable hematopoiesis characterized by a mild, normocytic anemia, and a progenitor pool that was slightly biased toward granulopoiesis (Fig. 6, A and B).

p57 deletion phenocopies TGFβ blockade during hematopoietic regeneration after chemotherapy

To assess the role of p57 in the TGFβ-mediated restoration of HSPC quiescence after chemotherapy, we administered 5FU to chimeric mice engrafted with p57-WT or p57-KO HSPCs, and then followed hematopoietic regeneration (Fig. 6 C). Mice with p57-KO hematopoiesis recovered BM and spleen cellularity and peripheral blood counts more rapidly compared with control mice engrafted with p57-WT hematopoiesis (Fig. 6, D–G; and unpublished data). Thus, similar to TGFβ signaling, p57 restrains hematopoietic recovery after BM stress. Importantly, our results show that the phenotype of p57-KO hematopoiesis is context dependent being mild during steady-state hematopoiesis and substantial during hematopoietic regeneration.

We next used multidimensional flow cytometry to determine whether shifts in HSPC populations explained why deletion of p57 helped to restore hematopoiesis after chemotherapy. At steady state, we found no significant difference in the HSPC populations but on day 15 after chemotherapy, at a time that TGFβ signaling and p57 expression are normally up-regulated, we found significantly more LKS^+ cells in mice with p57-KO hematopoiesis (Fig. 7, A–D). Similar effects were seen in the spleen (unpublished data). We functionally validated the expansion of immature HSPCs/multipotent

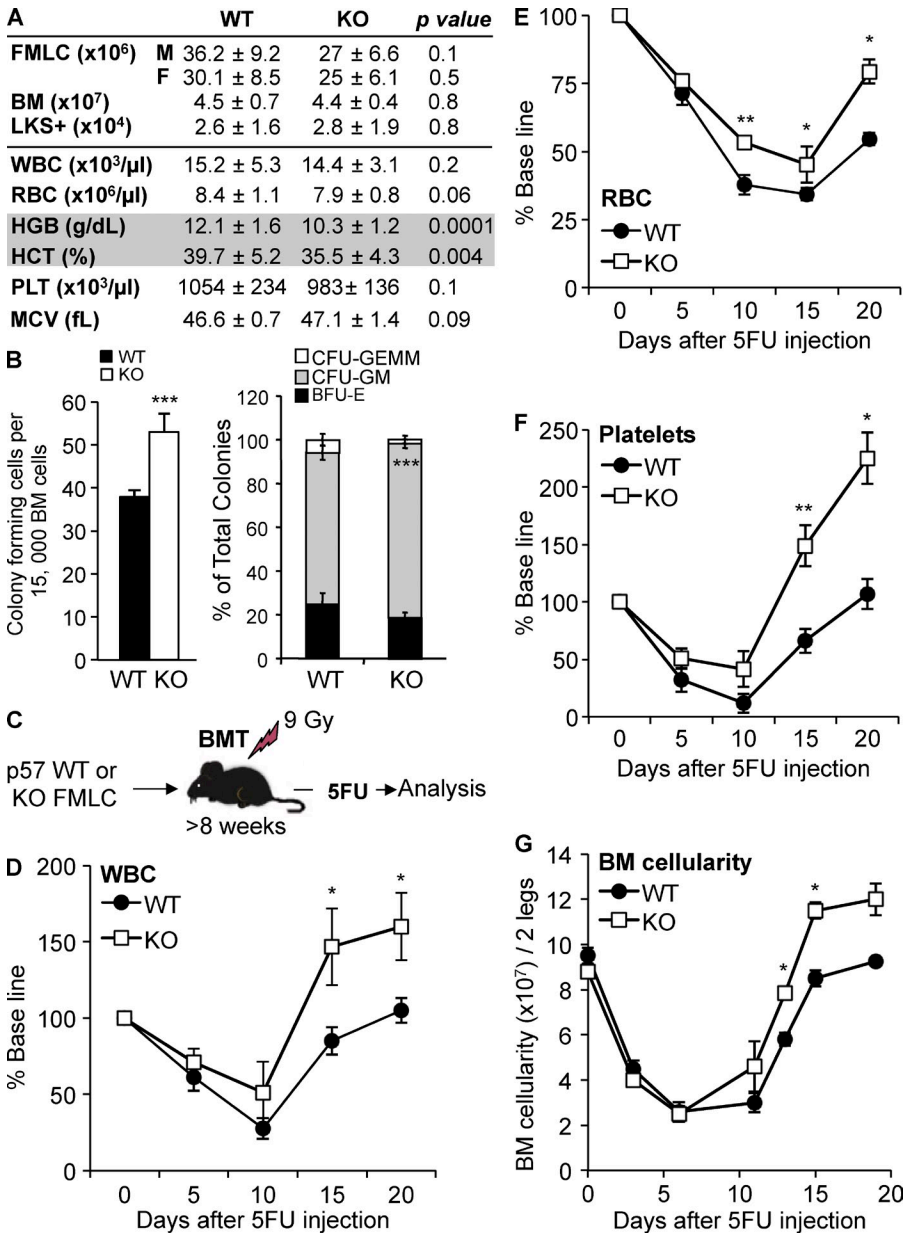

A		WT	KO	*p value*
FMLC (x10⁶)	M	36.2 ± 9.2	27 ± 6.6	0.1
	F	30.1 ± 8.5	25 ± 6.1	0.5
BM (x10⁷)		4.5 ± 0.7	4.4 ± 0.4	0.8
LKS+ (x10⁴)		2.6 ± 1.6	2.8 ± 1.9	0.8
WBC (x10³/µl)		15.2 ± 5.3	14.4 ± 3.1	0.2
RBC (x10⁶/µl)		8.4 ± 1.1	7.9 ± 0.8	0.06
HGB (g/dL)		12.1 ± 1.6	10.3 ± 1.2	0.0001
HCT (%)		39.7 ± 5.2	35.5 ± 4.3	0.004
PLT (x10³/µl)		1054 ± 234	983± 136	0.1
MCV (fL)		46.6 ± 0.7	47.1 ± 1.4	0.09

Figure 6. p57-KO HSPCs recover more robustly after myelosuppressive chemotherapy. (A) Table comparing hematologic parameters for p57-WT and p57-KO hematopoiesis. FLMCs were harvested from littermates and transplanted into lethally irradiated (9 Gr) C57BL/6 recipients to assess adult hematopoiesis. Once steady-state hematopoiesis was reached (≥12 wk), BM LKS^+ cells were enumerated by flow cytometry and normalized to cells per leg ($n = 5$ for each genotype). Blood cell counts ($n = 20$) are shown for WT and KO-transplanted mice after they reached homeostasis (>12 wk). BM, total BM cellularity, WBC, white blood cells; RBC, red blood cells; HGB, hemoglobin; HCT, hematocrit; PLT, platelets; MCV, Mean Corpuscular Volume. (B) CFC assay for committed HPCs is shown for chimeric mice with p57-WT (black bars) and p57-KO (white bars) BM cells. Total CFCs, CFU-GM (CFU-granulocyte, macrophage), CFU-GEMM (CFU-granulocyte, erythrocyte, macrophage, megakaryocyte), and BFU-E (Burst forming unit-erythroid) are presented in the graph ($n = 3$ in triplicate for each genotype). (C) Littermate FLMCs were isolated from p57-WT or p57-KO embryos and transplanted into lethally irradiated C57BL/6J recipient mice ($n = 10$). Once homeostasis was reached (~10 wk), recipient mice were treated with a single myelosuppressive dose of 5FU (150 mg/kg, i.p) as indicated. Peripheral blood WBCs (D), RBCs (E), platelets (F), and BM cellularity (G) are shown for chimeric mice with p57-WT (black circles) and p57-KO (white squares) hematopoiesis. All quantified data are shown as mean ± SEM (*, $P < 0.05$; **, $P < 0.01$; ***, $P < 0.001$, or if undesignated, the comparison was not significant).

progenitors (MPPs) by analyzing spleen colony-forming units (CFU-S) before and after chemotherapy (Fig. 7 E; McCulloch, 2002). These results suggest that without p57, immature HSPCs undergo additional rounds of cell division during BM regeneration.

We assessed the cell cycle status of p57-KO and p57-WT HSPCs in untreated, homeostatic BM and during recovery from myelosuppressive chemotherapy. We found a small, but statistically significant reduction in the number of quiescent LKS$^+$ cells in p57-KO chimeric mice (Fig. 7 G, D0). Steady state quiescence is thought to protect HSCs from cell cycle active agents such as 5FU, and more actively cycling HSCs, such as those deficient in p21 (Cdkn1a), are sensitized to the cytotoxic effects of 5FU (Cheng et al., 2000b). However,

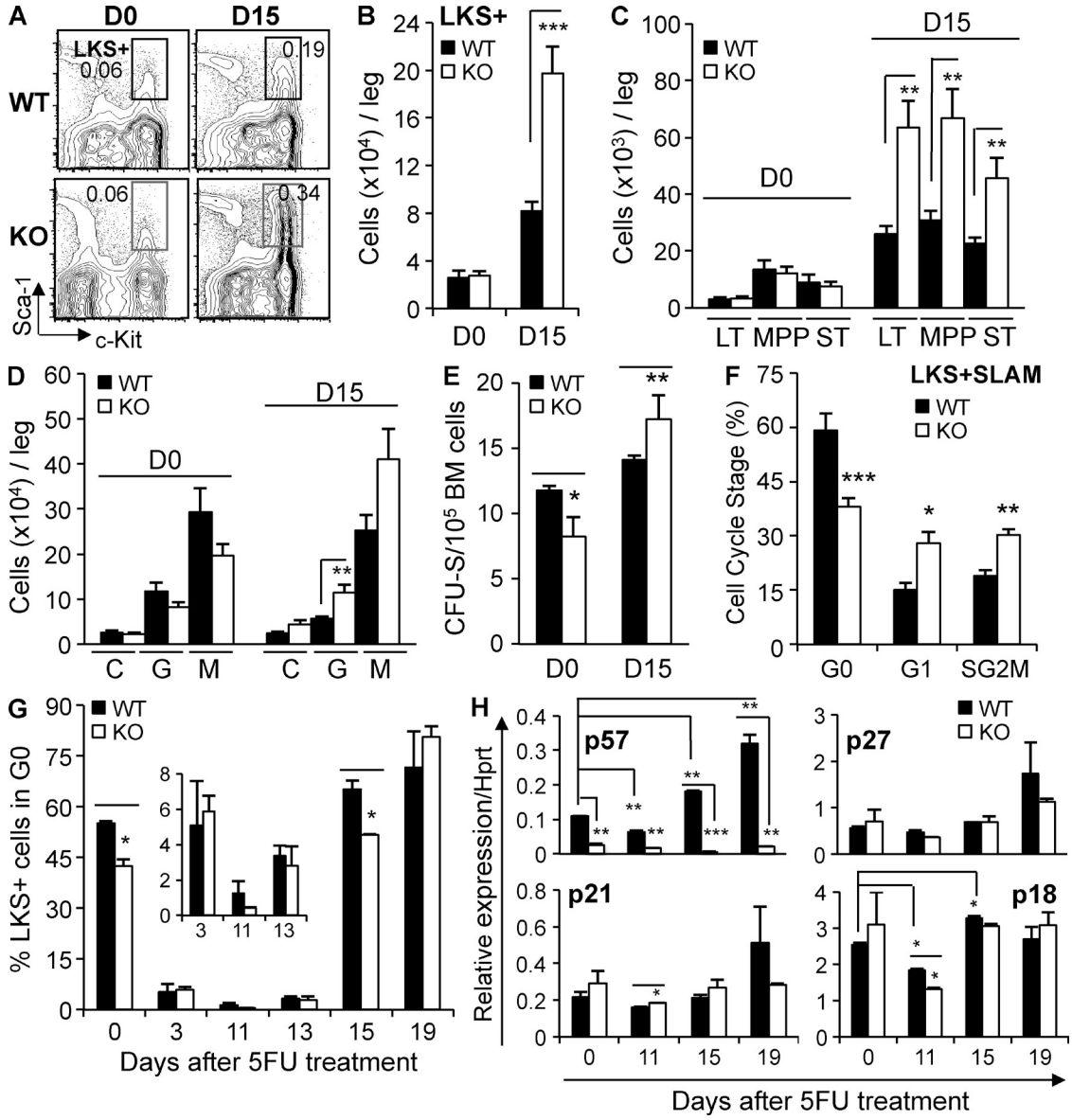

Figure 7. p57-KO hematopoiesis phenocopies inhibition of TGFβ signaling during BM regeneration. (A) Representative multidimensional flow cytometry of p57-WT and p57-KO BM LKS$^+$ cells is shown before treatment (D0) and day 15 after treatment with 5FU (frequency in total BM). (B and C) Flow cytometric enumeration of LKS$^+$ (Lin$^-$cKit$^+$Sca1$^+$) cells, and LKS$^+$Flk2$^-$CD34$^-$ (LT), LKS$^+$Flk2$^-$CD34$^+$ (ST), LKS$^+$Flk2$^+$CD34$^+$ (MPP) subpopulations (n = 5) is shown before (D0) and during hematopoietic regeneration (D15). (D) Immunophenotypic CMP (C), GMP (G) and MEP (M) is shown before (D0) and after (D15) chemotherapy (n = 5). (E) Expansion of immature MPPs was functionally validated using the CFU-S assay (n = 3). (F) Bi-dimensional cell cycle analysis is shown for p57-KO LKS + SLAM cells isolated during regeneration (D15) from chimeric mice with p57-WT (black bars) or p57-KO (white bars) hematopoiesis. (G) The population of quiescent LKS$^+$ cells before treatment (D0) and at various times after treatment with 5FU is shown. (H) Expression of *p57*, *p21*, *p18*, and *p27* mRNA in Lin$^-$ BM cells of p57-WT and p57-KO recipients was assessed by qRT-PCR before and at the indicated times after chemotherapy administration. Expression was normalized to *Hprt1* at each time point (n = 3). All quantified data are shown as mean ± SEM (*, P < 0.05; **, P < 0.01; ***, P < 0.001, or if undesignated, the comparison was not significant).

chimeric mice with p57-KO hematopoiesis appeared no more sensitive to 5FU than those with p57-WT hematopoiesis as assessed by the collinear decline of blood counts (Fig. 6, D–F), and BM cellularity (Fig. 6 G) immediately after chemotherapy (day 0 to 3). During recovery from myelosuppressive chemotherapy, p57 deletion delays the return to quiescence of LKS^+ cells and LKS + SLAM HSCs (Fig. 7, F and G), but LKS^- hematopoietic progenitors return to quiescence on time (unpublished data). This delay allows greater expansion of HSPCs and faster hematopoietic recovery. Thus, the hematopoietic phenotype of p57 deletion is remarkably similar to the effect of TGFβ blockade during recovery from hematopoietic stress.

Although the cytostatic effects of TGFβ appear to require p57 induction in WT hematopoietic cells, other CDKIs may partially compensate for p57 deletion in our engineered mouse strain (Zou et al., 2011). We quantified the relative mRNA expression of CDKIs known to affect HSC function in immature hematopoietic cells purified from mice engrafted with p57-WT or p57-KO HSCs. We did not identify basal (day 0) differences between p57-KO and p57-WT chimeric mice in the expression of p21, p27 or p18 suggesting that these other CDKIs do not compensate for deletion of p57 in the knockout strain that we studied (Zhang et al., 1997; Fig. 7 H). More importantly, we found no stress-induced changes in the expression of CDKIs other than p57 could explain the phenotype of mice with p57-KO hematopoiesis, suggesting that these effects are specific to p57. These results indicate that p57 safeguards HSC quiescence during homeostasis and helps restore quiescence during hematopoietic regeneration.

TGFβ blockade during recovery from hematopoietic stress delays HSC quiescence

Because the TGFβ–p57 axis induces HSCs to return to quiescence after myelosuppressive chemotherapy, we wondered if this pathway served a similar role in restoring homeostasis after other hematopoietic stresses. We used phenylhydrazine (PHZ) to trigger massive hemolysis and to recruit HSCs into cell cycle. To see if p57 functions in the restoration of HSC quiescence after hemolysis, we treated chimeric mice that were stably engrafted with p57-KO or p57-WT hematopoiesis with PHZ, and then analyzed the cell cycle of BM LKS + SLAM cells on day 8 (Fig. 8 A). During recovery from acute hemolysis, LKS + SLAM cells from mice with p57-KO hematopoiesis delayed their return to quiescence when compared with WT controls. Similarly, we found that TGFβ blockade with 1D11 (I) after acute hemolysis delayed the return of LKS + SLAM cells to quiescence when compared with mice treated with the 13C4 control antibody (C; Fig. 8 B). Whether we blocked TGFβ signaling by neutralizing the ligand (1D11) or by genetically deleting its downstream mediator (p57-KO), red blood cell counts recovered more quickly after hemolysis (Fig. 8 C). Next, we used LPS to model overwhelming infection to see if TGFβ signaling also restored HSC quiescence in this setting (Fig. 8 D). LKS + SLAM cells from mice that received a single dose of 1D11 after LPS had significantly prolonged cycling, implicating TGFβ signaling as a trigger—inducing quiescence during recovery from infection (Fig. 8, D and E). We also studied how TGFβ blockade altered the kinetics of HSC cycling after syngeneic BM transplantation (BMT) using lethal irradiation as conditioning. We transplanted recipient mice with 2 million BM cells from WT donors, and then administered 1D11 (I) or 13C4 (C) every 2–3 d between day 5 and 14 before sacrificing the recipients on day 19 for cell cycle analysis (Fig. 8 F). As in other stressors, a greater proportion of LKS + SLAM cells were actively cycling when TGFβ signaling was blocked during recovery from the hematopoietic stress of engraftment. Significantly, blood counts recovered more quickly when TGFβ signaling was inhibited during engraftment (Fig. 8, G–I). Thus, the TGFβ–p57 axis is commonly used to reestablish HSC quiescence during recovery from hematopoietic stress.

Hematopoietic stress provides p57-KO HSCs with a context-dependent competitive advantage

We examined the possibility that p57-KO HSPCs are inherently proliferative by competitively transplanting C57BL/6J recipient mice with a 1:1 mixture of congenic CD45.1 FLMCs and either p57-WT or p57-KO littermate $CD45.2/EGFP^+$ FLMCs (Fig. 9 A). We then monitored multilineage engraftment in the blood of the recipient animals for 6 mo. Unlike p18-KO HSCs, which progressively overrun WT HSCs (Yuan et al., 2004), p57-KO cells do not unreservedly self-renew during steady-state hematopoiesis; in fact, we found them slightly underrepresented compared with their littermate p57-WT controls (Fig. 9 B). This difference is not the result of imbalanced early engraftment because p57-WT and p57-KO cells lodge in and home to the marrow of recipient mice with equal efficiency 2, 24, and 48 h after transplantation (unpublished data).

Interfering with TGFβ signaling after chemotherapy delays the return to quiescence and permits additional rounds of HSPC cell division during hematopoietic regeneration. Chimeric mice with p57-KO hematopoiesis partially phenocopy this delay because genetic deletion of p57 in HSCs extinguishes this module of TGFβ-mediated signaling in the context of hematopoietic recovery. To test the durability of this stress-induced cycling, we administered chemotherapy to mice after competitively engrafting them with p57-KO or p57-WT HSCs and allowing them to reach steady state (~10 wk; see Materials and methods). We then monitored the relative contribution of each genotype—marked by CD45 isotypes and EGFP—during recovery from myelotoxic stress (Fig. 9 C). The proportion of p57-WT test cells remained constant during recovery from chemotherapy (black bars). This is the expected result because p57-WT ($CD45.2/EGFP^+$) test cells differ from the congenic p57-WT ($CD45.1/EGFP^-$) control cells only in their expression of marker genes. In striking contrast, the proportion of p57-KO test cells rose ~2-fold by day 11 after chemotherapy, and this effect persisted for almost 7 wk (the longest time point we analyzed). This result demonstrates that HSPCs

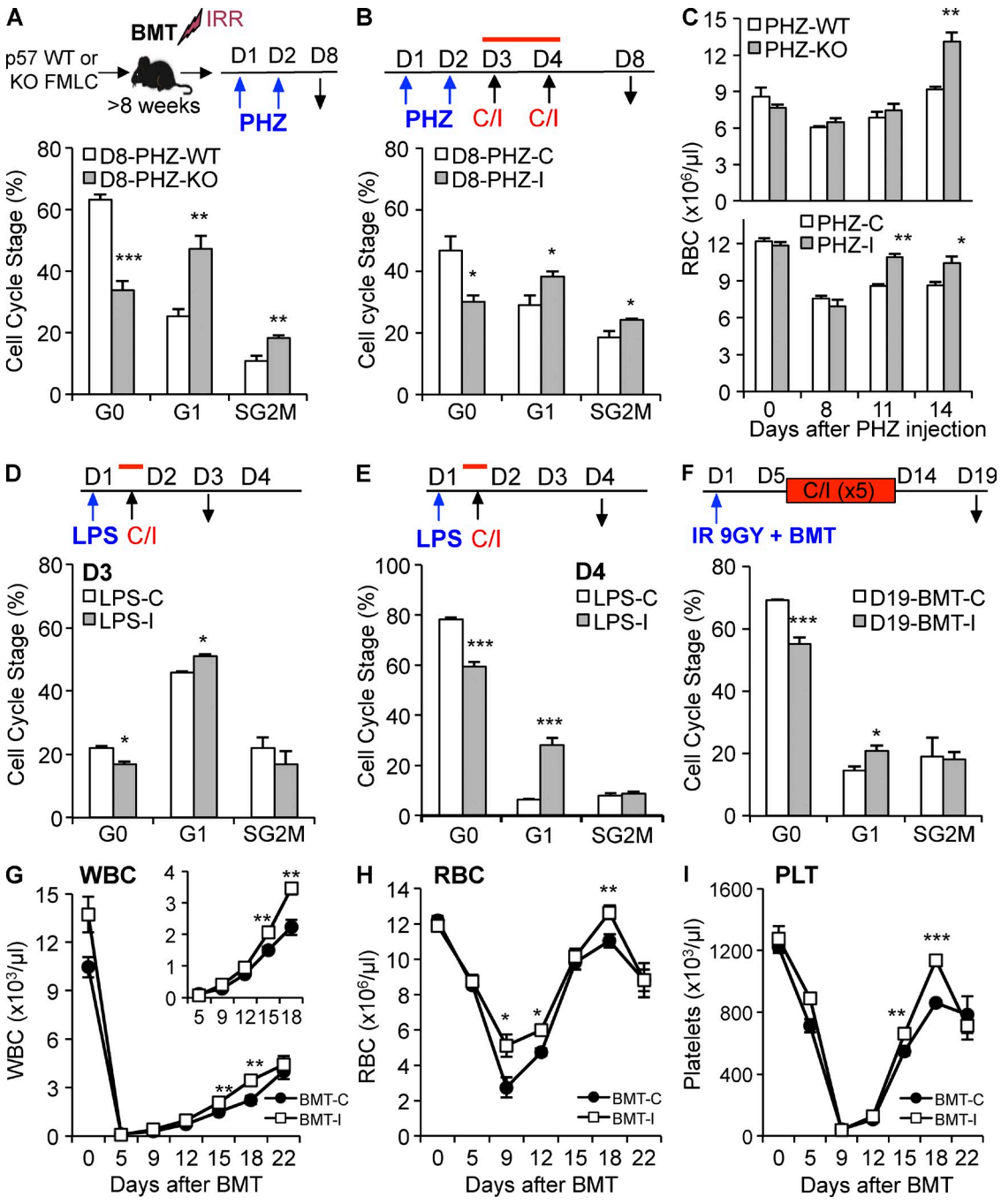

Figure 8. Blockade of TGFβ during recovery from hematologic stress prolongs HSPC cycling. (A) Chimeric mice with p57-WT or p57-KO hematopoiesis were injected with phenylhydrazine hydrochloride (PHZ) on day 1 and 2, and then killed on day 8 for LKS + SLAM cell cycle analysis. (B) C57BL/6J mice were injected with PHZ as previously described, and then with either the TGFβ-neutralizing antibody 1D11 (PHZ-I) or control antibody 13C4 (PHZ-C) on day 3 and 4 before analysis on day 8. (C) Chimeric mice with either p57-WT or p57-KO hematopoiesis (top) and C57BL/6J mice (bottom) were treated with PHZ as described, and RBC recovery was monitored during recovery. (D and E) C57BL/6J mice were injected with LPS on day 1, and then with either 1D11 (LPS-I) or 13C4 (LPS-C) 6 h later. Cell cycle status of LKS + SLAM cells was analyzed on day 3 (D) and 4 (E) after LPS administration. (F–I) Lethally irradiated mice were transplanted with 2×10^6 WT BM cells on day 1 and administered either 1D11 (BMT-I) or 13C4 (BMT-C) on day 7, 9, 11, and 14 after transplantation. Mice were sacrificed on day 19 for LKS + SLAM cell cycle analysis (F). Recovery of blood WBCs (G), RBCs (H), and PLTs (I) was monitored over time for transplanted mice treated with either 1D11 (BMT-I, white squares) or 13C4 (BMT-C, black circles). All quantified data are shown as mean ± SEM (*, $P < 0.05$; **, $P < 0.01$; ***, $P < 0.001$, or if undesignated, the comparison was not significant).

unable to induce p57 during hematopoietic regeneration have a cell-intrinsic competitive advantage that persists until homeostasis is reestablished. Once homeostasis returns, the p57-KO HSPCs maintain a fixed, albeit expanded, contribution to hematopoiesis.

Our data suggest that blockade of TGFβ-induced cytostasis during recovery could be used to limit chemotherapy-induced myelosuppression. One concern, however, is that blocking TGFβ will delay the up-regulation of p57 and permit HSPC cycling to continue, thereby sensitizing hematopoiesis to repeated chemotherapy treatments. We tested this possibility by treating chimeric mice stably engrafted with p57-WT or p57-KO HSCs with monthly doses of severely myelosuppressive chemotherapy. Whereas three cycles of chemotherapy killed half of the control mice, all mice with p57-KO hematopoiesis survived (Fig. 9 D).

DISCUSSION

We show that spatiotemporally constrained activation of TGFβ signaling in HSPCs helps restore homeostasis after myelosuppressive chemotherapy, and blocking TGFβ after chemotherapy delays homeostasis and accelerates multilineage hematopoietic reconstitution. These results provide the first evidence that hematopoietic homeostasis is actively reimposed during recovery from myelotoxic stress and suggest that blocking TGFβ activation to delay homeostasis could be an effective strategy to limit chemotherapy-induced myelosuppression.

HSCs are predominantly quiescent, but they can be rapidly recruited into cell cycle by hematologic stresses such as chemotherapy, infection, or bleeding. These triggers set off a remarkable adaptation that sacrifices HSPC quiescence, and the protection it affords, to meet an urgent need for new blood cell production. Growth factors clearly drive HSPC

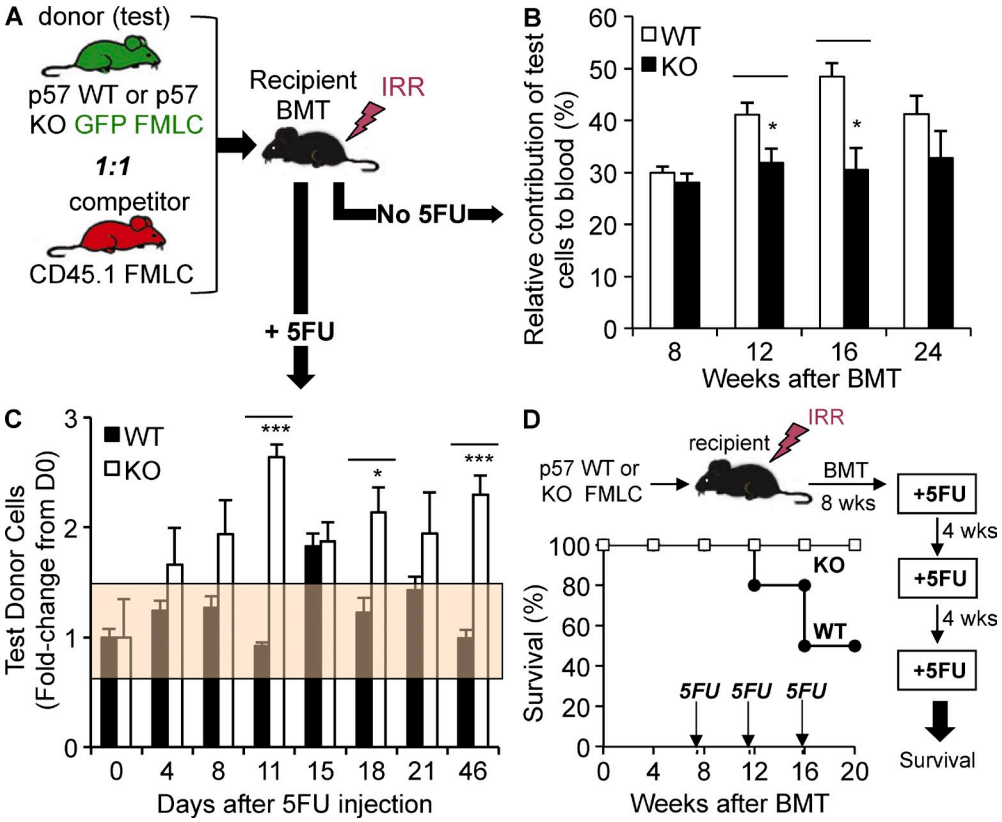

Figure 9. Hematopoietic stress confers a competitive advantage to p57-KO HSCs. (A) Schematic representation of competitive repopulation analysis. CD45.1$^+$ control FLMCs were mixed 1:1 with a test population of either p57-WT or p57-KO FLMCs (EGFP$^{+/+}$), and then transplanted into lethally irradiated recipient mice (n = 10). Stably engrafted mice with p57-WT or p57-KO hematopoiesis were analyzed at steady state (B) or after chemotherapy (C). (B) Multilineage peripheral blood engraftment was analyzed by flow cytometry at the indicated times after reconstitution to assess the proportion of p57-WT or p57-KO cells (n = 10). (C) To study the effect of myelosuppressive stress in competitively transplanted recipient mice, recipients were allowed to reach homeostasis (10 wk), and then given a single dose of myelosuppressive chemotherapy. Multilineage engraftment was assessed as described previously to monitor the relative contribution of p57-WT or p57-KO hematopoiesis during regeneration (n = 10). The percentage of donor cells was normalized to the day 0 measure for each mouse. The orange box represents the standard deviation of the day 0 measurements. (D) Kaplan-Meier survival curve is shown for chimeric mice stably engrafted with p57-WT or p57-KO hematopoiesis (n = 10), and then cyclically treated every 4 wk with a myelosuppressive dose of 5FU. All quantified data are shown as mean ± SEM (*, P < 0.05; **, P < 0.01; ***, P < 0.001, or if undesignated, the comparison was not significant).

mobilization and proliferation during stress, yet, once the hematopoietic demands have been adequately met, hematopoiesis must return to homeostasis. We have found that the TGFβ pathway helps restore quiescence and that its downstream target, p57, is a central mediator of this effect.

We propose a model of context-dependent TGFβ activity during hematopoietic regeneration. At steady state (homeostasis), most HSCs are maintained in a quiescent state by niche factors such as TPO, Ang1/2, and possibly TGFβ. During early stress, HSCs are mobilized from the niche and actively cycle throughout early regeneration, during which cytopenias persist and HSPCs proliferate to repopulate the BM. TGFβ signaling is then activated to reimpose HSPC quiescence during late regeneration, once hematopoiesis has sufficiently recovered. Transient blockade of TGFβ during late regeneration permits HSPCs to undergo additional rounds of division while the inhibitor concentration wanes. In the absence of p57, the cytostatic activity of TGFβ is delayed but eventually other, seemingly less potent, TGFβ targets reestablish quiescence. Whereas hematologic stress sacrifices HSC quiescence to meet an urgent hematopoietic demand, context-dependent TGFβ signaling is deployed to safeguard against HSC exhaustion once the excess demand has been adequately met.

Although many cell types produce TGFβ, it is secreted as a latent protein in noncovalent complex with the latency-associated peptide (LAP) that prevents it from binding to TGFβ receptors. In turn, LAP interacts with members of the latent TGFβ-binding protein (LTBP) family that can moor the large latent complex in the extracellular matrix. LTBPs influence the release of TGFβ from LAP—a process called activation—to allow TGFβ-mediated signaling via cell surface TGFβ receptors (Annes et al., 2003). Latent TGFβ is activated by several mechanisms. LAP can be shed after cleavage by matrix metalloproteinases, or plasmin, or through conformational changes induced by reactive oxygen species or adhesive interactions with thrombospondin-1 (TSP1) and integrins (e.g., $\alpha v\beta 6$ and $\alpha v\beta 8$; Sato et al., 1990; Barcellos-Hoff and Dix, 1996; Crawford et al., 1998; Munger et al., 1998, 1999; Ribeiro et al., 1999; Yu and Stamenkovic, 2000; Mu et al., 2002; Yang et al., 2007). These diverse mechanisms of TGFβ activation likely underlie the context-dependent, downstream biological effects of TGFβ, but little is known about how they function in hematopoiesis. Large quantities of latent TGFβ are incorporated into bone matrix (Pfeilschifter et al., 1998). Nonetheless, few BM cells show significant TGFβ signaling during steady-state hematopoiesis (Yamazaki et al., 2011), suggesting that critical aspects of this signaling are regulated by the availability of active TGFβ to its cellular receptors. We found that active TGFβ levels increase significantly during late hematopoietic regeneration. This raises the possibility that BM remodeling during recovery from chemotherapy could be responsible for context-dependent activation of matrix-associated latent TGFβ. Indeed, professional bone remodeling osteoclasts are induced during hematopoietic stress and can activate latent bone-associated TGFβ (Kollet et al., 2006; Tang et al., 2009; Wu et al., 2010). Further elucidation of the mechanisms responsible for prereceptor, spatiotemporal activation of TGFβ in BM will be important for understanding the context-dependent activity of TGFβ in hematopoiesis.

We show that context-dependent TGFβ signaling reestablishes HSPC quiescence. To our knowledge, this is the first demonstration of counterregulation dampening hematopoietic regeneration. Notably, feedback inhibition by soluble factors, including TGFβ was recently shown to restrict cytokine-driven proliferation of HSPCs in vitro (Csaszar et al., 2012). Future and prior work studying TGFβ in hematopoiesis must be evaluated with this context-dependent signaling in mind because hematopoietic phenotypes observed after transplantation, chemotherapy delivery, or MX-Cre induction with interferon are all expected to induce HSC stress that is eventually dampened by TGFβ signaling. For instance, genetic deletion of p57 was recently linked to altered HSC quiescence during homeostasis (Matsumoto et al., 2011; Zou et al., 2011), but the experimental systems used for these studies induce transient hematopoietic stress and, predictably, TGFβ activation (Tesio and Trumpp, 2011). We found that the effects of TGFβ are mediated in part by induction of p57. It is difficult to directly compare our studies of p57 with these prior reports because of significant differences in the studies performed. For instance, the murine model generated by the Nakayama group (Yan et al., 1997; Takahashi et al., 2000), and used by the Suda group (Zou et al., 2011), has a milder phenotype than the strain we used (Zhang et al., 1997), perhaps owing to the compensatory up-regulation of p27 observed in that strain (Zou et al., 2011) but not seen in ours. Significantly, our studies have potential clinical relevance and suggest that TGFβ blockade after chemotherapy may be an effective strategy to minimize multilineage myelosuppression.

Our results show that TGFβ blockade during recovery acts by delaying homeostasis and thereby accelerating hematopoietic regeneration. One obvious consideration is that prolonging HSPC cycling in this way could sensitize hematopoiesis to cyclic chemotherapy. Nonetheless, we found that p57 deletion did not increase the toxicity of monthly myelosuppressive chemotherapy. This may be because genetic deletion of p57 simply delays homeostasis but does not prevent other aspects of TGFβ signaling, or other mechanisms of counterregulation, to eventually reestablish HSPC quiescence. Thus, the effects of p57 deletion during regeneration appear transient. Supporting this notion, we found that p57 deletion allows HSPCs to outcompete those with intact p57 only during recovery from chemotherapy, and this advantage dissipates once homeostasis is reestablished. Thus, it is unlikely that p57 is the only downstream mediator of TGFβ signaling during hematopoietic regeneration. Indeed, the effect of TGFβ blockade on recovery from chemotherapy appeared stronger than that we observed in chimeric mice with p57-KO hematopoiesis.

Disruption of TGFβ signaling in hematopoietic cells has been achieved by knockout of its cognate receptors, disturbing the function of receptor-activated Smads or overexpressing

inhibitory Smads. Curiously, these approaches yield widely disparate hematopoietic phenotypes. Whereas HSCs seem indifferent to the presence of Tgfbr1 (Larsson et al., 2003), genetic deletion of Smad4 (Karlsson et al., 2007) or of Tgfbr2 predisposes HSCs to exhaustion cautioning against long-term TGFβ blockade (Yamazaki et al., 2011). Yet disruption of TGFβ signaling by overexpression of Smad7 promotes HSC self-renewal suggesting that, in some contexts, TGFβ inhibition can promote regeneration (Blank et al., 2006). Whether these discrepancies can be explained by noncanonical TGFβ signaling in the absence of Tgfbr2 remains to be clarified (Iwata et al., 2012). Our data suggests that the specific timing of TGFβ blockade is also important and that short-term inhibition of TGFβ during hematopoietic regeneration need not have the same consequences as permanent ablation of signaling via genetic knockouts.

Currently, GCSF is used to promote granulocytic recovery after myelosuppressive chemotherapy. Our results show that blocking the counterregulatory signals that dampen hematopoietic recovery is a potentially superior way to promote multilineage hematopoietic regeneration. This finding is important because TGFβ pathway inhibitors are currently in clinical development as direct antineoplastics because they can limit micro-metastases and prevent epithelial–mesenchymal transformation (Muraoka et al., 2002; Yang et al., 2002; Yingling et al., 2004; Biswas et al., 2007). This raises the tantalizing possibility that TGFβ blockade after cytotoxic chemotherapy could enhance antitumor activity while minimizing potentially dose-limiting myelotoxicity.

MATERIALS AND METHODS

Animals. Mice with targeted disruption of the p57 gene (Zhang et al., 1997) were backcrossed into C57BL/6J (The Jackson Laboratory). Mice with homozygous deletion of p57 (i.e., $p57^{-/-}$ or p57-KO mice) or with a maternally inherited p57-targeted allele ($p57^{+/-}$m) are not viable but embryos survive to at least day 20 (E20) allowing FLMCs to be harvested from viable embryos. To facilitate analysis of HSC transplant recipient mice, we crossed p57 mice with transgenic mice expressing EGFP under control of the ubiquitin C promoter (Schaefer et al., 2001). Hematopoietic cells from these mice express EGFP in all blood lineages. Chimeric p57-WT and p57-KO mice were generated by transplanting C57BL/6J mice with FLMCs harvested from littermate embryos (E15.5). Chimeric mice engrafted for 10–16 wk before analysis to permit hematopoiesis to reach steady-state. Animals were maintained in the Weill Cornell Medical College Animal Facility. All protocols were approved by the Weill Cornell Medical College Institutional Animal Care and Use Committee.

Immunophenotypic analysis of BM HSPCs and HSCs by flow cytometry. Mice were killed by CO_2 asphyxiation and femur, tibia, and humeri were dissected free of muscle and tendons and crushed in DMEM using a mortar and pestle. The resulting cell suspension was filtered through a 70-µm mesh and washed in PEB (2 mM EDTA, 0.2% BSA in PBS, pH 7.4). Spleens were isolated, and then minced before grinding through a 70-µm mesh to generate single-cell suspensions. Lin^- cells were purified using a biotinylated lineage cell depletion cocktail (Miltenyi Biotec). Lineage-depleted cells were then stained with streptavidin-Qdot 605 (eBioscience), Horizon V450-conjugated anti-CD117 (BD), PECy7-conjugated Sca-1 (BioLegend), Alexa Fluor 700-conjugated CD34 (BD), APC-conjugated CD135 (Flk2; BioLegend), and PerCP/Cy5.5-conjugated CD16/32 (FcR). Hematopoietic populations were identified as following: LT-HSCs, LKS+ $CD34^-Flk2^-$; short-term HSCs, LKS^+ $CD34^+$ $Flk2^-$; MPPs, LKS^+ $CD34^+$ $Flk2^+$; common myeloid progenitors (CMPs), LKS^- $CD34^+$ FcRlow; granulocyte macrophage progenitors (GMPs), LKS^- $CD34^+$ FcR^+; and megakaryocyte erythroid progenitors (MEPs), LKS^- $CD34^-$ FcR^- MEPs. DAPI was used to exclude dead cells during flow cytometric analysis. To identify LKS + SLAM cells, lineage-depleted cells were stained with APC-conjugated CD117 (BD), PECy7-conjugated Sca-1 (BioLegend), Alexa Fluor 700–conjugated CD48 (BioLegend) and PE-conjugated CD150 (BioLegend). To analyze cell cycle, lineage-depleted cells were stained with streptavidin-PE (BioLegend), APC-conjugated CD117 (BD), and PECy7-conjugated Sca-1 (BioLegend), and then fixed and permeabilized using CytoFix/Perm (BD) before staining with PerCP/C5.5-conjugated Ki67 (BD) and Hoechst 33342 (Invitrogen). The cell cycle status of LKS + SLAM cells was analyzed using this same strategy. Analysis gates were set based upon the fluorescence minus one (FMO) fluorophore. Multidimensional FACS analysis was performed using a BD LSRII equipped with five lasers (BD). FlowJo was used to analyze flow cytometry data (Tree Star).

Stem and progenitors cell assays. Primitive myeloid progenitors were enumerated using the day 12 CFU-S assay. In brief, recipient mice were irradiated and injected with 10^5 BM cells. Spleens were isolated 12 d after transplantation and fixed in Bouin's solution. The number of macroscopic spleen colonies were counted and expressed as the number of CFU-S colonies per 10^5 donor cells. Clonogenic myeloid progenitors were assessed by standard methylcellulose CFC assays (MethoCult GF M3434; Stem Cell Technologies) using 1.5×10^4 BM mononuclear cells (BMMCs) per well (6-well plate). Colonies were scored after 7 d of incubation and expressed as the number of CFUs per 1.5×10^4 BMMCs.

HSC transplantation. Recipient mice were irradiated with 9 Gy using a ^{137}Cs-γ-ray source. 3–4 h after lethal irradiation, FLMCs or BMMCs from donor animals were injected into the tail vein of recipient animals. For competitive repopulation assessing p57 function, either p57-WT or p57-KO test FLMCs ($EGFP^{+/+}$) were mixed with the same number of control FLMCs from congenic $CD45.1^{+/+}$ pups. The 1:1 (test/competitor) mixture (10^6 cells total) was injected into lethally irradiated mice via tail vein ($n = 10$). Peripheral blood was analyzed by flow cytometry at various times after reconstitution for the presence of p57-WT or p57-KO $CD45.2^{+/+}$, $EGFP^{+/+}$ cells test cells and $EGFP^{-/-}$ $CD45.1^{+/+}$ control cells. Multilineage engraftment was assessed by the proportion of $EGFP^+$ erythrocytes and by the proportion of cells in gates with specific side-scatter versus CD45, EGFP, and forward-scatter profiles corresponding to granulocytes and lymphocytes. The lineage within these gates was confirmed by staining for Gr1 and CD3.

To assess how TGFβ blockade during hematopoietic regeneration affects functional HSC activity, we competitively transplanted WT recipient mice with mixtures of genetically marked cells ($EGFP^{+/+}$, $CD45.2^{+/+}$ or $EGFP^{-/-}$, $CD45.1^{+/+}$) isolated from the BM of mice treated with 5FU, and then with either the TGFβ-neutralizing antibody 1D11 (I) or a nontargeted control antibody 13C4 (C; see Myelosuppressive treatment and TGFβ inhibition). On day 15, BM cells for each condition (D15-C or D15-I) were isolated and mixed 1:1 (2×10^6 cells total), and then injected into lethally irradiated C57BL/6J mice via tail vein ($n = 10$). Peripheral blood was analyzed for multilineage engraftment by flow cytometry at various times after transplantation. The origin of donor cells was identified by the EGFP, CD45.2, and CD45.1 staining profiles. To control for any influence of the genetic marker (none observed), we performed the experiment in two cohorts: one with a mixture of $EGFP^{+/+}$-D15-I and $CD45.1^{+/+}$-D15-C BMMCs and a second with a mixture of $EGFP^{+/+}$-D15-C and $CD45.1^{+/+}$-D15-I BMMCs.

Myelosuppressive treatment. We used 5FU (250 mg/kg; 1 i.p.) for C57BL/6J mice, or 5FU 150 mg/kg (1 i.p.) for mice that had been previously transplanted. To assess blood count recovery, we collected peripheral blood (50 µl) into EDTA-coated capillary tubes (Thermo Fisher Scientific).

Differential blood counts were measured using an automated ADVIA 120 Multispecies Hematology Analyzer (Bayer HealthCare) calibrated for murine blood.

TGFβ inhibition. We treated cohorts of mice with 5FU on day 0, and then with either the TGFβ-neutralizing antibody 1D11 (I; 10 mg/kg) or a nontargeted control antibody 13C4 (C; 10 mg/kg) on day 5, 7, and 9. The 1D11 and 13C4 antibodies were provided by Genzyme. Hematopoietic reconstitution was followed by monitoring peripheral blood counts and multidimensional flow cytometry on BM and spleen cells, as indicated.

Other hematologic stressors. To induce hemolysis, C57BL/6J mice or chimeric mice stably engrafted with p57-WT or p57-KO FLMCs were injected with phenylhydrazine hydrochloride (PHZ; 60 mg/kg, i.p; Sigma-Aldrich) on day 1 and 2. To assess the function of TGFβ signaling, C57BL/6J mice were treated with either the TGFβ-neutralizing antibody 1D11 (I; 10 mg/kg) or a nontargeted control antibody 13C4 (C; 10 mg/kg) on day 3 and 4 after PHZ. Mice were sacrificed on day 8 for analysis. As a model of massive infection, C57BL/6J mice were injected with LPS (2 mg/kg, i.p.; Sigma-Aldrich), and with either I or C 6 h after LPS, and then sacrificed on day 3 and 4 for analysis. To assess the effect of TGFβ blockade on HSC function after transplantation, we lethally irradiated mice (9 Gy), and then transplanted them with 2×10^6 BM cells from 8-wk-old C57BL/6J donor mice. Next, we injected recipient mice with either I or C every 2 to 3 d between day 5 and 14 after transplantation. Mice were sacrificed on day 19 for analysis. The effect of these treatments on the return of HSCs to quiescence was assessed by analyzing the bivariate cell cycle of LKS-SLAM cells isolated from the BM of recipient mice.

BM homing. BM cells were harvested from donor chimeric mice engrafted with $EGFP^{+/+}$ p57-WT or p57-KO hematopoiesis. Recipients were conditioned by lethal irradiation, and then transplanted with 10 million donor BM cells. Lodgement and engraftment of donor cells was analyzed at 2, 24, and 48 h after transplantation. Recipients were killed by CO_2 asphyxiation and donor LKS^+ cells were identified in recipient BM by flow cytometry.

TGFβ measurement. Mice were killed by CO_2 asphyxiation and the femurs were dissected free of muscle and tendons, and then crushed in PEB (2 mM EDTA, 0.2% BSA in PBS pH 7.4) using a mortar and pestle. The resulting cell suspension was filtered through a 70-µm filter and remaining cells and particulates were removed by centrifugation. The clarified supernatant was used to quantify total and active TGFβ1 by ELISA (R&D Systems) following the manufacturer's instructions.

IHC and IF. Femurs were fixed in 4% PFA overnight, and then decalcified using 10% EDTA before freezing in OCT (Sakura Finetek). IHC staining was performed on frozen sections using anti-pSmad2 (EMD Millipore) and anti-p57 (Epitomics) antibodies. The specificity of staining was assessed in sequential sections using nontargeted, species-matched, primary antibodies in place of the pSmad2 or p57 antibodies. After blocking endogenous peroxidase with 0.1% hydrogen peroxide, sections were incubated in primary antibodies overnight at 4°C, followed by signal amplification using Avidin-Biotin horseradish peroxidase complex method (ABC VECTASTAIN; Vector Laboratories). The time used for color development was fixed for all conditions. Sections were briefly counterstained with Methyl Green (Vector Laboratories). Staining was quantified by collecting images from 20 high-power fields per masked slide. The images were then independently analyzed by two blinded reviewers. For IF staining, cells were sorted using a 5-laser FACSAria II Special Research instrument (BD) and collected onto Cell-Tak (BD)–coated coverslips before fixation with 4% PFA. Cells were permeabilized with 0.1% Triton X-100, blocked in PBS, 2% BSA, and 5% normal donkey serum (NDS) and incubated overnight with pSmad2 (EMD Millipore) and/or p57 (Epitomics) antibodies. Cells were then stained with donkey anti–goat Alexa Fluor 488 and/or donkey anti–rabbit Alexa Fluor 555 and counterstained with DAPI to reveal nuclei. Coverslips were mounted in 70% glycerol and images were collected using a Zeiss 710 laser scanning confocal microscope. For quantitative analysis of p57 and pSmad2 positive cells, fluorescence intensity was quantified using ImageJ software (National Institutes of Health [NIH]).

Immunoblotting. BM or spleen cells were depleted of lineage-expressing cells, and then washed and pelleted before lysis in TBS containing 2 mM EDTA, 1X Laemmli Sample Buffer, 1% NP-40, with phosphatase inhibitors (10 mM sodium fluoride, 1 mM sodium pyrophosphate) and protease inhibitor cocktail tablets (Roche). Samples were separated on 10% NuPAGE gels (Invitrogen), and transferred to polyvinylidene difluoride (PVDF) membranes (EMD Millipore) before blocking with 5% nonfat dried milk in PBS with 0.1% Tween-20. Primary and secondary antibodies were diluted in blocking solution. Primary antibodies against p57 (Epitomics), p27 (BD), pSmad2 (EMD Millipore) Smad 2/3 (gift from J. Massagué, Memorial Sloan-Kettering Cancer Center, New York, NY), and β-actin (Cell Signaling Technology) were used. Secondary peroxidase-conjugated anti–rabbit antibody (EMD Millipore) was used before chemiluminescent visualization using the SuperSignal West Femto Substrate (Thermo Fisher Scientific). Signal intensities were quantified using ImageJ (NIH).

Quantitative RT-PCR analysis. Transcript expression was analyzed by reverse transcription quantitative PCR (qPCR) using a 7500 Fast Real-Time PCR System with a TaqMan Fast Universal PCR master mixture (Applied Biosystems). Expression was normalized to Hprt1 (Mm00446968_m1). Standard curves were generated with FLMC RNA from WT mice. The following TaqMan Gene Expression Assay Mixes were used: p57 (Mm00438170_m1), p21 (Mm00432448_m1), p18 (Mm00483243_m1), and p27 (Mm00438168_m1)

Statistical analysis. Student's *t* test (two-tailed) was used to analyze the statistical differences between groups, with the p-values indicated in the related graphs. All data are expressed as mean ± SEM (*, $P < 0.05$; **, $P < 0.01$; ***, $P < 0.001$).

Online supplemental material. Figure S1 shows the flow cytometric gating strategy. Online supplemental material is available at http://www.jem.org/cgi/content/full/jem.20121610/DC1.

The authors extend special thanks to Drs. Peter Besmer and Joan Massagué (Memorial Sloan-Kettering Cancer Center [MSKCC]) and to Drs. Ralph Nachman and Todd Evans (Weill Cornell Medical College [WCMC]) for critically reviewing the manuscript and for their considerable support. We also thank Genzyme Corp. for providing the 1D11 and 13C4 antibodies. We appreciate the help provided by Dr. Agnès Viale and Magali Cavatore from the MSKCC Genomics Core Laboratory, Steve Merlin (WCMC) for assistance with cell sorting, Drs. Elisa de Sanchina and Huiyong Zhao from the MSKCC Antitumor Assessment Core Laboratory, and Dr. Bi-Sen Ding (WCMC) for help with confocal microscopy.

This work was funded in part by a National Cancer Institute grant (CA104082) and by a generous contribution of the Belfer Family.

The authors declare no competing financial interests.

Submitted: 19 July 2012
Accepted: 14 January 2013

REFERENCES

Annes, J.P., J.S. Munger, and D.B. Rifkin. 2003. Making sense of latent TGFbeta activation. *J. Cell Sci.* 116:217–224. http://dx.doi.org/10.1242/jcs.00229

Barcellos-Hoff, M.H., and T.A. Dix. 1996. Redox-mediated activation of latent transforming growth factor-beta 1. *Mol. Endocrinol.* 10:1077–1083. http://dx.doi.org/10.1210/me.10.9.1077

Batard, P., M.N. Monier, N. Fortunel, K. Ducos, P. Sansilvestri-Morel, T. Phan, A. Hatzfeld, and J.A. Hatzfeld. 2000. TGF-(beta)1 maintains hematopoietic immaturity by a reversible negative control of cell cycle and induces CD34 antigen up-modulation. *J. Cell Sci.* 113:383–390.

Biswas, S., M. Guix, C. Rinehart, T.C. Dugger, A. Chytil, H.L. Moses, M.L. Freeman, and C.L. Arteaga. 2007. Inhibition of TGF-beta with neutralizing antibodies prevents radiation-induced acceleration of metastatic cancer progression. *J. Clin. Invest.* 117:1305–1313. http://dx.doi.org/10.1172/JCI30740

Blank, U., and S. Karlsson. 2011. The role of Smad signaling in hematopoiesis and translational hematology. *Leukemia.* 25:1379–1388. http://dx.doi.org/10.1038/leu.2011.95

Blank, U., G. Karlsson, J.L. Moody, T. Utsugisawa, M. Magnusson, S. Singbrant, J. Larsson, and S. Karlsson. 2006. Smad7 promotes self-renewal of hematopoietic stem cells. *Blood.* 108:4246–4254. http://dx.doi.org/10.1182/blood-2006-02-005611

Bradford, G.B., B. Williams, R. Rossi, and I. Bertoncello. 1997. Quiescence, cycling, and turnover in the primitive hematopoietic stem cell compartment. *Exp. Hematol.* 25:445–453.

Capron, C., C. Lacout, Y. Lécluse, V. Jalbert, H. Chagraoui, S. Charrier, A. Galy, A. Bennaceur-Griscelli, E. Cramer-Bordé, and W. Vainchenker. 2010. A major role of TGF-beta1 in the homing capacities of murine hematopoietic stem cell/progenitors. *Blood.* 116:1244–1253. http://dx.doi.org/10.1182/blood-2009-05-221093

Cheng, T., N. Rodrigues, D. Dombkowski, S. Stier, and D.T. Scadden. 2000a. Stem cell repopulation efficiency but not pool size is governed by p27(kip1). *Nat. Med.* 6:1235–1240. http://dx.doi.org/10.1038/81335

Cheng, T., N. Rodrigues, H. Shen, Y. Yang, D. Dombkowski, M. Sykes, and D.T. Scadden. 2000b. Hematopoietic stem cell quiescence maintained by p21cip1/waf1. *Science.* 287:1804–1808. http://dx.doi.org/10.1126/science.287.5459.1804

Cheng, T., H. Shen, N. Rodrigues, S. Stier, and D.T. Scadden. 2001. Transforming growth factor beta 1 mediates cell-cycle arrest of primitive hematopoietic cells independent of p21(Cip1/Waf1) or p27(Kip1). *Blood.* 98:3643–3649. http://dx.doi.org/10.1182/blood.V98.13.3643

Cheshier, S.H., S.J. Morrison, X. Liao, and I.L. Weissman. 1999. In vivo proliferation and cell cycle kinetics of long-term self-renewing hematopoietic stem cells. *Proc. Natl. Acad. Sci. USA.* 96:3120–3125. http://dx.doi.org/10.1073/pnas.96.6.3120

Crawford, S.E., V. Stellmach, J.E. Murphy-Ullrich, S.M. Ribeiro, J. Lawler, R.O. Hynes, G.P. Boivin, and N. Bouck. 1998. Thrombospondin-1 is a major activator of TGF-beta1 in vivo. *Cell.* 93:1159–1170. http://dx.doi.org/10.1016/S0092-8674(00)81460-9

Csaszar, E., D.C. Kirouac, M. Yu, W. Wang, W. Qiao, M.P. Cooke, A.E. Boitano, C. Ito, and P.W. Zandstra. 2012. Rapid expansion of human hematopoietic stem cells by automated control of inhibitory feedback signaling. *Cell Stem Cell.* 10:218–229. http://dx.doi.org/10.1016/j.stem.2012.01.003

Dickson, M.C., J.S. Martin, F.M. Cousins, A.B. Kulkarni, S. Karlsson, and R.J. Akhurst. 1995. Defective haematopoiesis and vasculogenesis in transforming growth factor-beta 1 knock out mice. *Development.* 121: 1845–1854.

Ehninger, A., and A. Trumpp. 2011. The bone marrow stem cell niche grows up: mesenchymal stem cells and macrophages move in. *J. Exp. Med.* 208: 421–428. http://dx.doi.org/10.1084/jem.20110132

Fortunel, N., J. Hatzfeld, L. Aoustin, P. Batard, K. Ducos, M.N. Monier, A. Charpentier, and A. Hatzfeld. 2000a. Specific dose-response effects of TGF-beta1 on developmentally distinct hematopoietic stem/progenitor cells from human umbilical cord blood. *Hematol. J.* 1:126–135. http://dx.doi.org/10.1038/sj.thj.6200021

Fortunel, N.O., A. Hatzfeld, and J.A. Hatzfeld. 2000b. Transforming growth factor-beta: pleiotropic role in the regulation of hematopoiesis. *Blood.* 96:2022–2036.

Gorelik, L., and R.A. Flavell. 2000. Abrogation of TGFbeta signaling in T cells leads to spontaneous T cell differentiation and autoimmune disease. *Immunity.* 12:171–181. http://dx.doi.org/10.1016/S1074-7613(00)80170-3

Heissig, B., K. Hattori, S. Dias, M. Friedrich, B. Ferris, N.R. Hackett, R.G. Crystal, P. Besmer, D. Lyden, M.A. Moore, et al. 2002. Recruitment of stem and progenitor cells from the bone marrow niche requires MMP-9 mediated release of kit-ligand. *Cell.* 109:625–637. http://dx.doi.org/10.1016/S0092-8674(02)00754-7

Iwata, J.-I., J.G. Hacia, A. Suzuki, P.A. Sanchez-Lara, M. Urata, and Y. Chai. 2012. Modulation of noncanonical TGF-β signaling prevents cleft palate in Tgfbr2 mutant mice. *J. Clin. Invest.* 122:873–885. http://dx.doi.org/10.1172/JCI61498

Karlsson, G., U. Blank, J.L. Moody, M. Ehinger, S. Singbrant, C.X. Deng, and S. Karlsson. 2007. Smad4 is critical for self-renewal of hematopoietic stem cells. *J. Exp. Med.* 204:467–474. http://dx.doi.org/10.1084/jem.20060465

Kiel, M.J., O.H. Yilmaz, T. Iwashita, O.H. Yilmaz, C. Terhorst, and S.J. Morrison. 2005. SLAM family receptors distinguish hematopoietic stem and progenitor cells and reveal endothelial niches for stem cells. *Cell.* 121:1109–1121. http://dx.doi.org/10.1016/j.cell.2005.05.026

Kollet, O., A. Dar, S. Shivtiel, A. Kalinkovich, K. Lapid, Y. Sztainberg, M. Tesio, R.M. Samstein, P. Goichberg, A. Spiegel, et al. 2006. Osteoclasts degrade endosteal components and promote mobilization of hematopoietic progenitor cells. *Nat. Med.* 12:657–664. http://dx.doi.org/10.1038/nm1417

Kopp, H.G., S.T. Avecilla, A.T. Hooper, S.V. Shmelkov, C.A. Ramos, F. Zhang, and S. Rafii. 2005. Tie2 activation contributes to hemangiogenic regeneration after myelosuppression. *Blood.* 106:505–513. http://dx.doi.org/10.1182/blood-2004-11-4269

Lapidot, T., and I. Petit. 2002. Current understanding of stem cell mobilization: the roles of chemokines, proteolytic enzymes, adhesion molecules, cytokines, and stromal cells. *Exp. Hematol.* 30:973–981. http://dx.doi.org/10.1016/S0301-472X(02)00883-4

Larsson, J., M.J. Goumans, L.J. Sjöstrand, M.A. van Rooijen, D. Ward, P. Levéen, X. Xu, P. ten Dijke, C.L. Mummery, and S. Karlsson. 2001. Abnormal angiogenesis but intact hematopoietic potential in TGF-beta type I receptor-deficient mice. *EMBO J.* 20:1663–1673. http://dx.doi.org/10.1093/emboj/20.7.1663

Larsson, J., U. Blank, H. Helgadottir, J.M. Björnsson, M. Ehinger, M.J. Goumans, X. Fan, P. Levéen, and S. Karlsson. 2003. TGF-beta signaling-deficient hematopoietic stem cells have normal self-renewal and regenerative ability in vivo despite increased proliferative capacity in vitro. *Blood.* 102:3129–3135. http://dx.doi.org/10.1182/blood-2003-04-1300

Larsson, J., U. Blank, J. Klintman, M. Magnusson, and S. Karlsson. 2005. Quiescence of hematopoietic stem cells and maintenance of the stem cell pool is not dependent on TGF-beta signaling in vivo. *Exp. Hematol.* 33:592–596. http://dx.doi.org/10.1016/j.exphem.2005.02.003

Letterio, J.J., A.G. Geiser, A.B. Kulkarni, H. Dang, L. Kong, T. Nakabayashi, C.L. Mackall, R.E. Gress, and A.B. Roberts. 1996. Autoimmunity associated with TGF-beta1-deficiency in mice is dependent on MHC class II antigen expression. *J. Clin. Invest.* 98:2109–2119. http://dx.doi.org/10.1172/JCI119017

Levéen, P., J. Larsson, M. Ehinger, C.M. Cilio, M. Sundler, L.J. Sjöstrand, R. Holmdahl, and S. Karlsson. 2002. Induced disruption of the transforming growth factor beta type II receptor gene in mice causes a lethal inflammatory disorder that is transplantable. *Blood.* 100:560–568. http://dx.doi.org/10.1182/blood.V100.2.560

Lévesque, J.P., and I.G. Winkler. 2011. Hierarchy of immature hematopoietic cells related to blood flow and niche. *Curr. Opin. Hematol.* 18:220–225. http://dx.doi.org/10.1097/MOH.0b013e3283475fe7

Lévesque, J.P., J. Hendy, Y. Takamatsu, P.J. Simmons, and L.J. Bendall. 2003. Disruption of the CXCR4/CXCL12 chemotactic interaction during hematopoietic stem cell mobilization induced by GCSF or cyclophosphamide. *J. Clin. Invest.* 111:187–196.

Matsumoto, A., S. Takeishi, T. Kanie, E. Susaki, I. Onoyama, Y. Tateishi, K. Nakayama, and K.I. Nakayama. 2011. p57 is required for quiescence and maintenance of adult hematopoietic stem cells. *Cell Stem Cell.* 9:262–271. http://dx.doi.org/10.1016/j.stem.2011.06.014

McCulloch, E.A. 2002. CFU-S. In Hematopoietic Stem Cell Protocols. C.A. Klug, and C.T. Jordan, editors. Humana Press, Inc., Totowa, NJ. 153-160.

Miyamoto, K., K.Y. Araki, K. Naka, F. Arai, K. Takubo, S. Yamazaki, S. Matsuoka, T. Miyamoto, K. Ito, M. Ohmura, et al. 2007. Foxo3a is essential for maintenance of the hematopoietic stem cell pool. *Cell Stem Cell.* 1:101–112. http://dx.doi.org/10.1016/j.stem.2007.02.001

Morrison, S.J., D.E. Wright, and I.L. Weissman. 1997. Cyclophosphamide/granulocyte colony-stimulating factor induces hematopoietic stem cells to proliferate prior to mobilization. *Proc. Natl. Acad. Sci. USA.* 94:1908–1913. http://dx.doi.org/10.1073/pnas.94.5.1908

Mu, D., S. Cambier, L. Fjellbirkeland, J.L. Baron, J.S. Munger, H. Kawakatsu, D. Sheppard, V.C. Broaddus, and S.L. Nishimura. 2002.

The integrin alpha(v)beta8 mediates epithelial homeostasis through MT1-MMP-dependent activation of TGF-beta1. *J. Cell Biol.* 157:493–507. http://dx.doi.org/10.1083/jcb.200109100

Munger, J.S., J.G. Harpel, F.G. Giancotti, and D.B. Rifkin. 1998. Interactions between growth factors and integrins: latent forms of transforming growth factor-beta are ligands for the integrin alphavbeta1. *Mol. Biol. Cell.* 9:2627–2638.

Munger, J.S., X. Huang, H. Kawakatsu, M.J. Griffiths, S.L. Dalton, J. Wu, J.F. Pittet, N. Kaminski, C. Garat, M.A. Matthay, et al. 1999. The integrin alpha v beta 6 binds and activates latent TGF beta 1: a mechanism for regulating pulmonary inflammation and fibrosis. *Cell.* 96:319–328. http://dx.doi.org/10.1016/S0092-8674(00)80545-0

Muraoka, R.S., N. Dumont, C.A. Ritter, T.C. Dugger, D.M. Brantley, J. Chen, E. Easterly, L.R. Roebuck, S. Ryan, P.J. Gotwals, et al. 2002. Blockade of TGF-beta inhibits mammary tumor cell viability, migration, and metastases. *J. Clin. Invest.* 109:1551–1559.

Oshima, M., H. Oshima, and M.M. Taketo. 1996. TGF-beta receptor type II deficiency results in defects of yolk sac hematopoiesis and vasculogenesis. *Dev. Biol.* 179:297–302. http://dx.doi.org/10.1006/dbio.1996.0259

Passegué, E., A.J. Wagers, S. Giuriato, W.C. Anderson, and I.L. Weissman. 2005. Global analysis of proliferation and cell cycle gene expression in the regulation of hematopoietic stem and progenitor cell fates. *J. Exp. Med.* 202:1599–1611. http://dx.doi.org/10.1084/jem.20050967

Petit, I., M. Szyper-Kravitz, A. Nagler, M. Lahav, A. Peled, L. Habler, T. Ponomaryov, R.S. Taichman, F. Arenzana-Seisdedos, N. Fujii, et al. 2002. G-CSF induces stem cell mobilization by decreasing bone marrow SDF-1 and up-regulating CXCR4. *Nat. Immunol.* 3:687–694. http://dx.doi.org/10.1038/ni813

Pfeilschifter, J., I. Diel, B. Scheppach, A. Bretz, R. Krempien, J. Erdmann, G. Schmid, N. Reske, H. Bismar, T. Seck, et al. 1998. Concentration of transforming growth factor beta in human bone tissue: relationship to age, menopause, bone turnover, and bone volume. *J. Bone Miner. Res.* 13:716–730. http://dx.doi.org/10.1359/jbmr.1998.13.4.716

Qian, H., N. Buza-Vidas, C.D. Hyland, C.T. Jensen, J. Antonchuk, R. Månsson, L.A. Thoren, M. Ekblom, W.S. Alexander, and S.E. Jacobsen. 2007. Critical role of thrombopoietin in maintaining adult quiescent hematopoietic stem cells. *Cell Stem Cell.* 1:671–684. http://dx.doi.org/10.1016/j.stem.2007.10.008

Ribeiro, S.M., M. Poczatek, S. Schultz-Cherry, M. Villain, and J.E. Murphy-Ullrich. 1999. The activation sequence of thrombospondin-1 interacts with the latency-associated peptide to regulate activation of latent transforming growth factor-beta. *J. Biol. Chem.* 274:13586–13593. http://dx.doi.org/10.1074/jbc.274.19.13586

Sato, Y., R. Tsuboi, R. Lyons, H. Moses, and D.B. Rifkin. 1990. Characterization of the activation of latent TGF-beta by co-cultures of endothelial cells and pericytes or smooth muscle cells: a self-regulating system. *J. Cell Biol.* 111:757–763. http://dx.doi.org/10.1083/jcb.111.2.757

Scandura, J.M., P. Boccuni, J. Massagué, and S.D. Nimer. 2004. Transforming growth factor beta-induced cell cycle arrest of human hematopoietic cells requires p57KIP2 up-regulation. *Proc. Natl. Acad. Sci. USA.* 101:15231–15236. http://dx.doi.org/10.1073/pnas.0406771101

Schaefer, B.C., M.L. Schaefer, J.W. Kappler, P. Marrack, and R.M. Kedl. 2001. Observation of antigen-dependent CD8+ T-cell/ dendritic cell interactions in vivo. *Cell. Immunol.* 214:110–122. http://dx.doi.org/10.1006/cimm.2001.1895

Sitnicka, E., F.W. Ruscetti, G.V. Priestley, N.S. Wolf, and S.H. Bartelmez. 1996. Transforming growth factor beta 1 directly and reversibly inhibits the initial cell divisions of long-term repopulating hematopoietic stem cells. *Blood.* 88:82–88.

Takahashi, K., K. Nakayama, and K. Nakayama. 2000. Mice lacking a CDK inhibitor, p57Kip2, exhibit skeletal abnormalities and growth retardation. *J. Biochem.* 127:73–83. http://dx.doi.org/10.1093/oxfordjournals.jbchem.a022586

Tang, Y., X. Wu, W. Lei, L. Pang, C. Wan, Z. Shi, L. Zhao, T.R. Nagy, X. Peng, J. Hu, et al. 2009. TGF-beta1-induced migration of bone mesenchymal stem cells couples bone resorption with formation. *Nat. Med.* 15:757–765. http://dx.doi.org/10.1038/nm.1979

Tesio, M., and A. Trumpp. 2011. Breaking the cell cycle of HSCs by p57 and friends. *Cell Stem Cell.* 9:187–192. http://dx.doi.org/10.1016/j.stem.2011.08.005

Wilson, A., and A. Trumpp. 2006. Bone-marrow haematopoietic-stem-cell niches. *Nat. Rev. Immunol.* 6:93–106. http://dx.doi.org/10.1038/nri1779

Wilson, A., E. Laurenti, G. Oser, R.C. van der Wath, W. Blanco-Bose, M. Jaworski, S. Offner, C.F. Dunant, L. Eshkind, E. Bockamp, et al. 2008. Hematopoietic stem cells reversibly switch from dormancy to self-renewal during homeostasis and repair. *Cell.* 135:1118–1129. http://dx.doi.org/10.1016/j.cell.2008.10.048

Wu, X., L. Pang, W. Lei, W. Lu, J. Li, Z. Li, F.J. Frassica, X. Chen, M. Wan, and X. Cao. 2010. Inhibition of Sca-1-positive skeletal stem cell recruitment by alendronate blunts the anabolic effects of parathyroid hormone on bone remodeling. *Cell Stem Cell.* 7:571–580. http://dx.doi.org/10.1016/j.stem.2010.09.012

Yamazaki, S., A. Iwama, S. Takayanagi, Y. Morita, K. Eto, H. Ema, and H. Nakauchi. 2006. Cytokine signals modulated via lipid rafts mimic niche signals and induce hibernation in hematopoietic stem cells. *EMBO J.* 25:3515–3523. http://dx.doi.org/10.1038/sj.emboj.7601236

Yamazaki, S., A. Iwama, S. Takayanagi, K. Eto, H. Ema, and H. Nakauchi. 2009. TGF-beta as a candidate bone marrow niche signal to induce hematopoietic stem cell hibernation. *Blood.* 113:1250–1256. http://dx.doi.org/10.1182/blood-2008-04-146480

Yamazaki, S., H. Ema, G. Karlsson, T. Yamaguchi, H. Miyoshi, S. Shioda, M.M. Taketo, S. Karlsson, A. Iwama, and H. Nakauchi. 2011. Nonmyelinating Schwann cells maintain hematopoietic stem cell hibernation in the bone marrow niche. *Cell.* 147:1146–1158. http://dx.doi.org/10.1016/j.cell.2011.09.053

Yan, Y., J. Frisén, M.H. Lee, J. Massagué, and M. Barbacid. 1997. Ablation of the CDK inhibitor p57Kip2 results in increased apoptosis and delayed differentiation during mouse development. *Genes Dev.* 11:973–983.

Yang, Y.-A., O. Dukhanina, B. Tang, M. Mamura, J.J. Letterio, J. MacGregor, S.C. Patel, S. Khozin, Z.-Y. Liu, J. Green, et al. 2002. Lifetime exposure to a soluble TGF-beta antagonist protects mice against metastasis without adverse side effects. *J. Clin. Invest.* 109:1607–1615.

Yang, Z., Z. Mu, B. Dabovic, V. Jurukovski, D. Yu, J. Sung, X. Xiong, and J.S. Munger. 2007. Absence of integrin-mediated TGFbeta1 activation in vivo recapitulates the phenotype of TGFbeta1-null mice. *J. Cell Biol.* 176:787–793. http://dx.doi.org/10.1083/jcb.200611044

Yaswen, L., A.B. Kulkarni, T. Fredrickson, B. Mittleman, R. Schiffman, S. Payne, G. Longenecker, E. Mozes, and S. Karlsson. 1996. Autoimmune manifestations in the transforming growth factor-beta 1 knockout mouse. *Blood.* 87:1439–1445.

Yilmaz, O.H., M.J. Kiel, and S.J. Morrison. 2006. SLAM family markers are conserved among hematopoietic stem cells from old and reconstituted mice and markedly increase their purity. *Blood.* 107:924–930. http://dx.doi.org/10.1182/blood-2005-05-2140

Yingling, J.M., K.L. Blanchard, and J.S. Sawyer. 2004. Development of TGF-beta signalling inhibitors for cancer therapy. *Nat. Rev. Drug Discov.* 3:1011–1022. http://dx.doi.org/10.1038/nrd1580

Yoshihara, H., F. Arai, K. Hosokawa, T. Hagiwara, K. Takubo, Y. Nakamura, Y. Gomei, H. Iwasaki, S. Matsuoka, K. Miyamoto, et al. 2007. Thrombopoietin/MPL signaling regulates hematopoietic stem cell quiescence and interaction with the osteoblastic niche. *Cell Stem Cell.* 1:685–697. http://dx.doi.org/10.1016/j.stem.2007.10.020

Yu, Q., and I. Stamenkovic. 2000. Cell surface-localized matrix metalloproteinase-9 proteolytically activates TGF-beta and promotes tumor invasion and angiogenesis. *Genes Dev.* 14:163–176.

Yuan, Y., H. Shen, D.S. Franklin, D.T. Scadden, and T. Cheng. 2004. In vivo self-renewing divisions of haematopoietic stem cells are increased in the absence of the early G1-phase inhibitor, p18INK4C. *Nat. Cell Biol.* 6:436–442. http://dx.doi.org/10.1038/ncb1126

Zhang, P., N.J. Liégeois, C. Wong, M. Finegold, H. Hou, J.C. Thompson, A. Silverman, J.W. Harper, R.A. DePinho, and S.J. Elledge. 1997. Altered cell differentiation and proliferation in mice lacking p57KIP2 indicates a role in Beckwith-Wiedemann syndrome. *Nature.* 387:151–158. http://dx.doi.org/10.1038/387151a0

Zou, P., H. Yoshihara, K. Hosokawa, I. Tai, K. Shinmyozu, F. Tsukahara, Y. Maru, K. Nakayama, K.I. Nakayama, and T. Suda. 2011. p57(Kip2) and p27(Kip1) cooperate to maintain hematopoietic stem cell quiescence through interactions with Hsc70. *Cell Stem Cell.* 9:247–261. http://dx.doi.org/10.1016/j.stem.2011.07.003